AGU PUBLICATIONS

Geochemistry, Geophysics, Geosystems

RESEARCH ARTICLE

10.1002/2014GC005636

Key Points:

- Twelve new (U-Th)/He eruption ages for Dominica ranging from ~3 to 700 ka
- Prolonged zircon histories suggest protracted storage and recycling
- Timescales of intra-oceanic arc magmatism are similar to continental arcs

Supporting Information:

- Howe_et_al_SupportingInformation
- Table S1
- Table S2
- Table S3
- Table S4

Correspondence to:
T. M. Howe,
t.howe@auckland.ac.nz

Citation:
Howe, T. M., A. K. Schmitt, J. M. Lindsay, P. Shane, and D. F. Stockli (2015), Time scales of intra-oceanic arc magmatism from combined U-Th and (U-Th)/He zircon geochronology of Dominica, Lesser Antilles, *Geochem. Geophys. Geosyst.*, *16*, 347–365, doi:10.1002/2014GC005636.

Received 24 OCT 2014
Accepted 14 JAN 2015
Accepted article online 20 JAN 2015
Published online 5 FEB 2015
Corrected 18 MAR 2015

This article was corrected on 18 MAR 2015. See the end of the full text for details.

Time scales of intra-oceanic arc magmatism from combined U-Th and (U-Th)/He zircon geochronology of Dominica, Lesser Antilles

T. M. Howe[1], A. K. Schmitt[2], J. M. Lindsay[1], P. Shane[1], and D. F. Stockli[3]

[1]School of Environment, University of Auckland, Auckland, New Zealand, [2]Department of Earth, Planetary, and Space Sciences, University of California, Los Angeles, California, USA, [3]Department of Geological Sciences, University of Texas at Austin, Austin, Texas, USA

Abstract The island of Dominica, located in the intra-oceanic Lesser Antilles arc, has produced a series of intermediate (mostly andesitic) lava domes and ignimbrites since the early Pleistocene. (U-Th)/He eruption ages from centers across the island range from ~3 to ~770 ka, with at least 10 eruptions occurring in the last 80 ka. Three eruptions occurred near the southern tip of Dominica (Plat Pays Volcanic Complex) in the past 15 ka alone. Zircon U-Th ages from individual centers range from near-eruption to secular equilibrium implicating protracted storage and recycling of zircons within the crust. Overlapping zircon crystallization peaks within deposits from geographically separated vents (up to 40 km apart) indicate that magma associated with separate volcanic edifices crystallized zircon contemporaneously. Two lava domes from the southern sector of the island display exclusively young zircon rim ages (<50 ka) with narrow crystallization peaks consistent with the construction of a new magma reservoir. The younging of eruption and crystallization ages implies that the magmatic foci leading to the construction of this reservoir have migrated southward, arc-parallel over time. Overall, our data support geochemical models for the ongoing construction of a silicic intrusive complex, consisting of varying amounts of crystal mush, beneath the island. U-Pb zircon ages <1–2 Ma indicate that accumulation of this complex is entirely Quaternary in age. Together zircon U-Th and U-Pb ages for Dominica suggest that the magmatic processes and time scales operating in intra-oceanic arcs are similar to those documented for continental arcs.

1. Introduction

Intra-oceanic subduction zones are widely considered to be the primary location where continental crust originates [e.g., *Taylor*, 1967; *Scholl and von Huene*, 2009]. To adequately assess continental growth rates, quantitative constraints on magmatic additions in arcs, composed of both erupted and intruded magmas, are required. Although the ratio of volcanic to plutonic components is often cited at 1:5 [e.g., *White et al.*, 2006; *de Silva and Gosnold*, 2007] highlighting the importance of the dominant subterranean component, this ratio remains poorly constrained [cf. *Ward et al.*, 2014]. The proximal volcanic component is usually quantifiable from surface mapping and dating in active arcs where outcrops of eruptive products are typically easily accessible. In contrast, the subterranean magmatism is largely hidden, unless uplifted and exhumed by erosion, a mechanism that is likely to erase the accompanying volcanic component. Hence, petrologic studies have focused on the crystal record in volcanic rocks to constrain time scales and processes in the magmatic roots where the duration of magma crystallization to a first order correlates with the size of the system. Zircon provides a valuable thermochemical record of pre-eruptive magmatic history due to its stability and ability to yield high-resolution crystallization ages which can constrain the longevity of the plutonic component associated with volcanic systems. Zircon crystal age distributions from individual eruptions of arc volcanoes in continental settings can span hundreds of thousands of years, revealing prolonged storage and recycling of crystals within their magmatic reservoirs [e.g., *Charlier et al.*, 2003; *Bachmann et al.*, 2007; *Wilson and Charlier*, 2009; *Claiborne et al.*, 2010b; *Storm et al.*, 2012; *Klemetti and Clynne*, 2014]. As there is little geophysical evidence for largely molten reservoirs in the upper continental crust [*Iyer et al.*, 1990], it has been suggested that these reservoirs thermally oscillate between partly molten and mostly crystalline subsolidus intrusions, leading to the concept of crystal mushes, rigid interlocking-crystal (>50–60%) frameworks that are periodically reactivated prior to eruption [*Mahood*, 1990; *Bachmann and Bergantz*, 2003; *Hildreth*, 2004; *Cooper and Kent*, 2014].

Time scales of intra-oceanic arc magmatism where preexisting (ancient) continental crust is absent have largely been studied in extinct arcs [*Schaltegger et al*., 2002; *Rioux et al*., 2007; *Smyth et al*., 2007; *Pedersen et al*., 2010], where the record of early stages of arc crustal formation may be incomplete due to uplift, erosion, and overprinting by later magmatic activity. Studies of young active intra-oceanic arcs can, therefore, provide complimentary insights into the early stages of arc crustal maturation. The evolution of silicic magmas in such settings has been attributed to either fractionation of a basaltic parent [e.g., *Wade et al*., 2005; *Brophy*, 2008; *Barker et al*., 2012], anatexis of silicic mid to upper crust [e.g., *Vogel et al*., 2004; *Tamura et al*., 2009], or to partial melting of lower crustal amphibolite [e.g., *Annen et al*., 2006]. Despite the concept that magmas have less time to stall and differentiate during passage through thin mafic crust characteristic of island arcs compared to thicker continental crust [*Tatsumi and Eggins*, 1995], many authors have posited the presence of silicic magma bodies beneath intra-oceanic volcanoes [e.g., *Halama et al*., 2006; *Turner et al*., 2012]. Moreover, long-lived intracrustal crystal mush zones have been invoked to explain heterogeneous crystal populations in silicic magmas from the Kermadec arc [*Barker et al*., 2012], not unlike those envisioned for continental arcs [e.g., *Cooper and Kent*, 2014]. Although zircon has been successfully used to quantify the duration of preeruptive magma accumulation in silicic arc volcanic systems in continental arcs (e.g., Mt. St. Helens [*Claiborne et al*., 2010b] and Lassen [*Klemetti and Clynne*, 2014]), such studies remain scarce for intra-oceanic arcs. On the island of St. Lucia, Lesser Antilles, *Schmitt et al*. [2010b] found evidence for protracted (>350 ka) zircon recycling, which displayed patterns similar to those reported in continental arc settings [e.g., *Claiborne et al*., 2010b; *Klemetti and Clynne*, 2014]. However, the mainly dacitic magmas of St. Lucia are unusually evolved for the Lesser Antilles, which is dominated by basalt and andesite [*Brown et al*., 1977; *Macdonald et al*., 2000]. Thus, it is uncertain under which conditions crystal mush zones form in intra-oceanic arcs, and if their longevity is equivalent to those of continental arc volcanoes.

The island of Dominica, Lesser Antilles, is characterized by dominantly Pleistocene to recent volcanism in a dense clustering of eruptive centers that produced mostly andesitic lavas and pyroclastic flow deposits [*Lindsay et al*., 2005a, 2005b; *Halama et al*., 2006; *Smith et al*., 2013]. Dominica thus differs from St. Lucia which has only one evolved (dacitic) volcanic complex. Zircon geochronology from multiple volcanic centers on the island can provide a broader view into the mechanisms and timescales associated with magmatic accumulation and differentiation in intra-oceanic arcs. To elucidate the relationship between the erupted and nonerupted magma inferred from the presence of zircon, it is important to link the timing of zircon crystallization with eruption ages. This can be achieved using combined U-Th and (U-Th)/He geochronology [*Schmitt et al*., 2010b]. (U-Th)/He is an ideal eruption geochronometer characterized by fast diffusion of the radiogenic daughter ^{4}He, which only begins to accumulate in the zircon after the system has reached the closure temperature at the time eruption.

In this study, we use combined U-Th and (U-Th)/He geochronology to determine a magma chronology for young volcanism on Dominica. This approach provides new insight into (1) the relations between volcanic deposits and subterranean magmatic systems; (2) the potential interconnectivity between individual volcanic systems at depth; and (3) the possibility of a laterally extensive crystal-mush zone beneath the island. Our study has implications for the longevity of magmatic systems in intra-oceanic arcs and proposes that the time scales and processes of evolved island arc magmatism are in some instances fundamentally similar to those in continental arcs.

1.1. Geologic Background

The island of Dominica (750 km^2 area) is located in the center of the Lesser Antilles arc (Figure 1a) which marks the westward subduction of the North American Plate beneath the Caribbean Plate. The overriding Caribbean Plate is considerably thickened and is thought to consist of oceanic crust with possible remnants of a mid-Cretaceous oceanic flood basalt province which formed the Caribbean Plateau [*Kerr et al*., 2003] and early Cenozoic accretionary wedge sediments from an ancestral subduction zone [*Macdonald et al*., 2000]. Geophysical studies suggest that the Lesser Antilles crust ranges in thickness from ~24 to >30 km [*Boynton et al*., 1979; *Christeson et al*., 2008; *Kopp et al*., 2011]. Seismic models indicate a three-layer crustal structure for the Caribbean Plate consisting from top to bottom of lavas and volcanogenic sediments (1–10 km), intermediate to felsic middle crust (10–20 km), and a plutonic lower crust (20–28 km) [*Kopp et al*., 2011].

The volcanic rocks exposed on Dominica can be subdivided into four main groups based on age [*Lindsay et al*., 2005b; *Smith et al*., 2013]: (1) Miocene (6.8–5.2 Ma); (2) Pliocene (3.7–1.8 Ma); (3) Older Pleistocene (1.8–

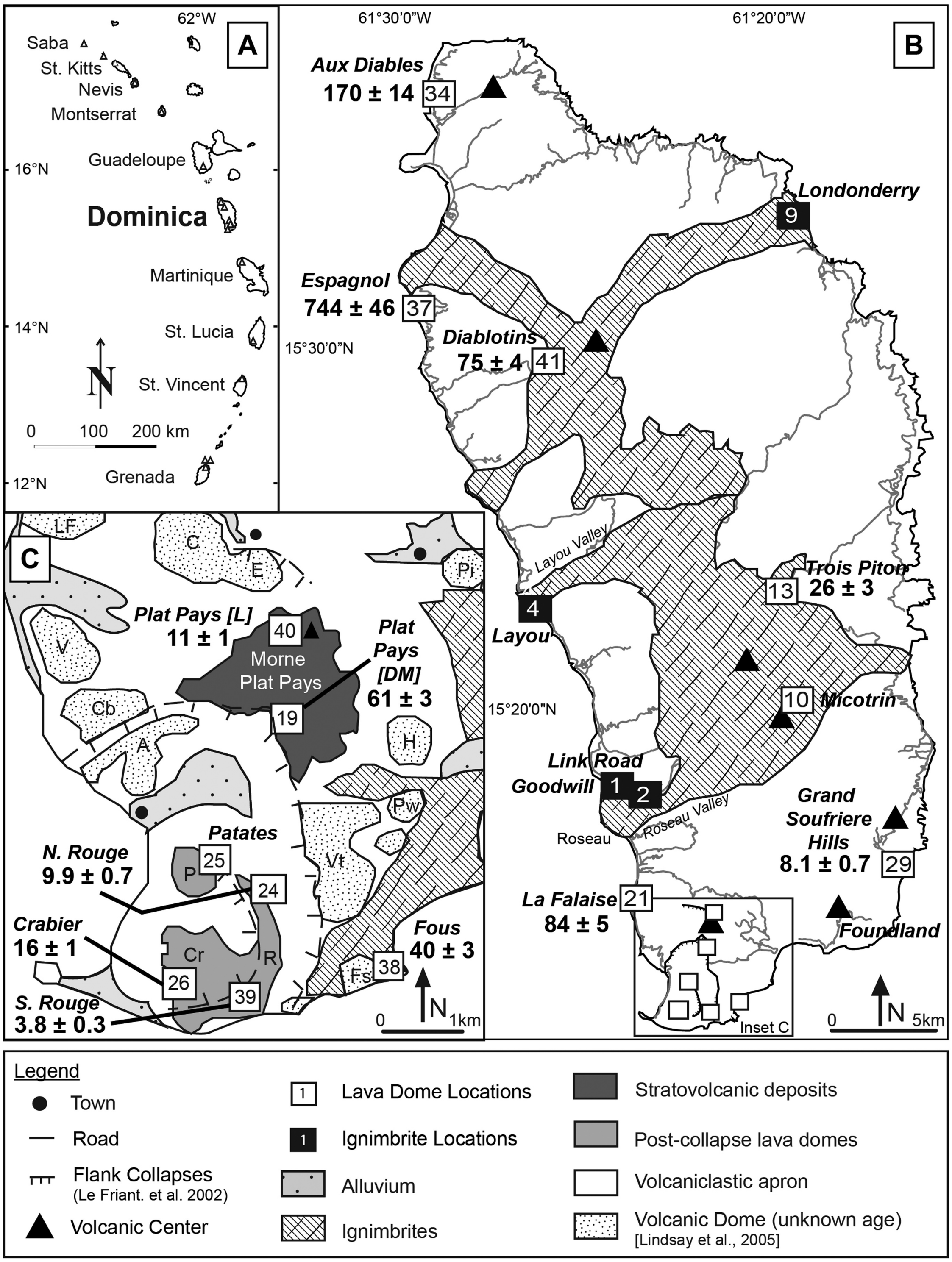

Figure 1. (a) Map of the Lesser Antilles island arc. (b) Map of Dominica showing sample locations detailed in Table 1 and the extent of ignimbrites (modified from *Smith et al.* [2013]). (U-Th)/He eruption ages $\pm 1\sigma$ are shown in bold. With the exception of Plat Pays [DM], these ages are considered very reliable. See section 3.1 for full explanation of the ages. (c) Simplified geologic map of the Plat Pays Volcanic Complex (PPVC). Volcanic deposits modified from *Lindsay et al.* [2003, 2005a]. Proposed collapse scarp locations taken from *Le Friant et al.* [2002]. Possible volcanic domes determined by *Lindsay et al.* [2005a] are designated by letters as follows: LF, La Falaise; C, Canot; V, LaVue/Vigie; A, Acouma; Cr, Crabier; R, Rouge; Vt, Vert; Pw, Powell; E, Elois; Cb, Cabrits; H, Hagley; Fs, Fous; Pi, Pichelin; P, Patates.

1.1 Ma); and (4) Younger Pleistocene to recent (1.1–present). Group 1 deposits outcrop on the eastern side of the island and consist of low-K basaltic complexes [*Bellon*, 1988; *Smith et al*., 2013]. Group 2 comprises large basaltic to andesitic stratovolcanoes which represent the initiation of more evolved volcanism on the island. Group 3 occurs in the northern half of Dominica and is associated with the development of Diablotins, a large andesitic stratovolcano, and the older parts of Aux Diables, a small Pelean dome complex (Figure 1) [*Smith et al*., 2013]. Group 4 deposits include younger deposits from Diablotins and Aux Diables and at least four coeval andesitic volcanic centers: Trois Piton, Micotrin, Grand Soufrière Hills, and the Plat Pays Volcanic Center (PPVC; Figure 1b). Radiometric ages for the Group 4 centers range from 450 years BP to >50 ka (Table 1). With the exception of the composite PPVC, each of these centers consists of a prominent central dome surrounded by parasitic domes and associated block-and-ash and pyroclastic flow deposits (Figure 1).

The PPVC is more complex than other centers and includes Morne Plat Pays, a large andesitic stratovolcano, and several smaller domes [*Lindsay et al*., 2003]. The primary volcanic stratigraphy of this center is thought to have been disturbed by three flank collapse events in the past 100 ka, which were identified by extensive debris avalanche deposits and two semicircular scarp structures [*Le Friant et al*., 2002]. One such event led to the development of the Soufrière Depression, a 3 km wide semicircular depression that truncates the western side of Morne Plat Pays (Figure 1c) [*Le Friant et al*., 2002]. Within the Soufrière Depression, topographic highs of unknown age have been variously described as domes [*Lindsay et al*., 2003, 2005a] or debris avalanche deposits [*Roobol et al*., 1983; *Le Friant et al*., 2002; *Samper et al*., 2008]. Only three small domes (Rouge, Crabier, and Patates) are unanimously identified as in situ post collapse volcanic edifices [*Le Friant et al*., 2002; *Lindsay et al*., 2005a; *Samper et al*., 2008]. Patates, dated at ~450–600 years old, is the youngest dome on the island [*Lindsay et al*., 2003].

Although Pleistocene-recent activity on Dominica has been dominated by Pelean dome-forming eruptions [*Lindsay et al*., 2005b; *Smith et al*., 2013], young pumiceous pyroclastic flow deposits also outcrop across the island. Such extensive ignimbritic deposits only exist on the central islands of the Lesser Antilles (Martinique, St. Lucia, and Dominica) and are uncommon in most intra-oceanic systems [*Macdonald et al*., 2000; *Leat and Larter*, 2003]. Major pyroclastic flow deposits include the Roseau Sequence [*Sigurdsson*, 1972; *Smith et al*., 2013; *Howe et al*., 2014], the Layou pyroclastic flow [*Whitham*, 1989], and the Wesley/Londonderry pyroclastic flow [*Smith et al*., 2013] (Figure 1b). Sourced from south-central Dominica, the Roseau Sequence represents six or seven eruptions that occurred between ~20 and 70 ka [*Howe et al*., 2014]. The Layou pyroclastic flow is thought to be sourced from the Trois Piton dome complex [*Smith et al*., 2013], and the Wesley/Londonderry pyroclastic flow has been associated with the Diablotins center [*Sparks et al*., 1980; *Smith et al*., 2013]. Limited exposure and tightly overlapping major and trace element compositions of whole-rock, glass, and minerals of most deposits prevent unambiguous identification of source volcanoes for any of the pumiceous pyroclastic flow deposits [*Smith et al*., 2013; *Howe et al*., 2014].

Several authors have attempted to determine the characteristics of the magma roots of Dominica with a specific focus on deposits from within the PPVC [*Gurenko et al*., 2005; *Lindsay et al*., 2005a; *Halama et al*., 2006]. Although *Lindsay et al*. [2005a] found little field evidence of mafic recharge within PPVC lava samples, *Halama et al*. [2006] proposed that andesitic to dacitic PPVC lavas are formed via injection and mixing of mafic magmas into a long-lived (>100 ka) shallow silicic reservoir. A broad compilation of whole-rock and mineral chemistry from centers across the island suggests that the majority of Dominica volcanic rocks contain chemically heterogeneous populations of crystals which have experienced varying thermal histories [*Smith et al*., 2013]. Based on this and the homogeneity of whole-rock major and trace element compositions, *Smith et al*. [2013] proposed the existence of an island wide, mid to upper crustal batholith beneath Dominica.

2. Materials and Methods

2.1. Samples and Mineral Separation

Fourteen lava samples from 10 separate domes and one pumice sample from each of five pyroclastic flow deposits were collected for this study (Figures 1b and 1c and Table 1). With the exception of Aux Diables and Morne Espagnol, all lava dome samples investigated here are medium-K, calc-alkaline andesites [*Lindsay et al*., 2005b; *Smith et al*., 2013]. The Aux Diables sample is a tholeiitic andesite, while the Morne Espagnol sample is from a small dacitic plug [*Smith et al*., 2013]. Pumices from the studied pyroclastic flow

Table 1. Sample Locations and Previous Age Dates for Dominica Dome and Pyroclastic Flow Deposits[a]

					Previous Ages		
Location No.	Unit Name	Coordinates	Location Description	Outcrop Type[b]	Original (Cal)	Method	Reference[c]
Northern Domes							
34	Aux Diables	N15°37.108	Small quarry south of Clifton	BA	>46,740	^{14}C[d]	1
		W61°27.812			43,710 ± 1,590 (45,398 ± 2,054)	^{14}C	1
37	Espagnol	N15°31.694	Northern side of dome	LF	2.24 ± 0.34 Ma	K-Ar	2
		W61°27.992					
41	Diablotins	N15°30.012	Along Kachibona Lake track	LB	>46,620	^{14}C	1
		W61°24.873			0.7 ± 0.5 Ma	K-Ar	3
					0.72 ± 0.11 Ma	K-Ar	4
Central Domes							
10	Micotrin	N15°20.459	Western edge of	LB	1,160 ± 45 (868 ± 68)	^{14}C	5
		W61°18.586	Freshwater Lake		26,500 ± 900 (29,247 ±757)	^{14}C	5
					25,370 ± 120 (28,253 ± 274)	^{14}C	5
13	Trois Piton	N15°23.367	Quarry on northern	BA	17,240 ± 720 (18,722 ± 913)	^{14}C	3
		W61°18.738	side of Trois Piton		25,310 ± 230 (28,230 ± 307)	^{14}C	6
29	Grand Soufríere Hills	N15°16.615	Quarry south of	BA	10,320 ± 40 (10,259 ± 171)	^{14}C	1
		W61°15.371	Point Mulatre		11,000 ± 85 (10,970 ± 112)	^{14}C	5
					0.8 ± 0.4 Ma[e]	^{14}C	3
Southern Domes (Outside Depression Margin)							
19	Plat Pays (Margin)	N15°14.161	North-eastern edge of	BA	6,600 ± 50 (5,555 ± 46)	^{14}C	7
		W61°20.608	Depression Margin		6,670 ± 70 (5,594 ± 54)	^{14}C	1
					6,825 ± 75 (5,732 ± 68)	^{14}C	8
40	Plat Pays [Mt. Lofty]	N15°15.347	North-western side of	LB	6,650 ± 50 (5,580 ± 40)	^{14}C	8
		W61°20.931	Plat Pays at Mt. Lofty estate				
21	La Falaise	N15°16.186	La Falaise quarry on	DAD	>47,330[e]	^{14}C	8
		W61°22.534	coast south of Loubiere		96,000 ± 2,000	K-Ar	9
38	Fous	N15°12.803	South-west edge of Morne Fous	LB			
		W61°20.233	behind Petit Coulibri estate				
Southern Domes (Inside Depression Margin)							
24	Northern Rouge	N15°13.457	Northern edge of Rouge Ridge	BA			
		W61°21.078					
25	Patates	N15°13.720	Road outcrop between	LB	450 ± 90[f] (510 ± 93)	^{14}C	6
		W61°21.173	Galion and Soufriere		685 ± 55 (635 ± 50)	^{14}C	8
26	Crabier	N15°12.788	South-western side of Crabier	LB			
		W61°21.592					
39	Southern Rouge	N15°12.763	Southern edge of Rouge Ridge	LB			
		W61°20.779					
Pyroclastic Flow Deposits							
1	Roseau Tuff (Unit I)	N15°18.506	Goodwill Quarry	I	62 ± 8 ka	(U-Th)/He	10
		W61°23.067					
2	Roseau Tuff	N15°18.256	Along Santa Romet Link Road	I	24.5 ± 2.0 ka	(U-Th)/He	10
	(Units II and III)	W61°22.465			34.7 ± 3.1 ka	(U-Th)/He	10
4	Layou Flow	N15°23.859	Coastal Road near the Layou River	I	65 ± 5 ka	(U-Th)/He	10
		W61°25.607					
9	Wesley Flow	N15°33.614	Londonderry Beach	I	80 ± 8 ka	(U-Th)/He	10
		W61°17.832					

[a]Numbers in column 1 refer to sample locations on Figure 1. All errors shown are 1σ.
[b]BA = block-and-ash flow deposit; LF = lava flow; LB = lava boulder; DAD = debris avalanche deposit; I = ignimbrite.
[c]References: 1, *Smith et al.* [2013]; 2, *Bellon* [1988]; 3, G. Wadge (unpublished report, 1989); 4, M. C. Monjaret (unpublished thesis 1985); 5, *Lindsay et al.* [2005a]; 6, *Roobol et al.* [1983]; 7, *Le Friant et al.* [2002]; 8, *Lindsay et al.* [2003]; 9, *Samper et al.* [2008]; 10, *Howe et al.* [2014].
[d]^{14}C ages are displayed with the original age followed by the calibrated age in parentheses. Ages were calibrated using CalPal online and the CalPal2007_HULU calibration curve and are thus in Cal years BP.
[e]Regarded as too old or suspect by previous authors.
[f]Thought to contain anthropogenic material (L. Honeychurch, personal communication, 2012).

deposits range in composition from andesite to dacite and are generally indistinguishable from the dome deposits in major and trace element geochemistry [*Smith et al.*, 2013; *Howe et al.*, 2014].

Zircons were separated using magnetic and heavy liquid separation as outlined in *Schmitt et al.* [2003]. At least 20 crystals from each sample were handpicked and mounted for analysis. Overall 447 U-Th and 50 U-Pb ages were determined on 460 crystal rims. A subset of zircons from each sample was then selected for (U-Th)/He analyses based on crystal size and morphology. A minimum of five aliquots per sample were prepared for He analysis. These analyses yielded 12 (U-Th)/He ages associated with 10 separate lava dome centers. (U-Th)/He ages for the pyroclastic units are presented in *Howe et al.* [2014] and referred to but not discussed here.

2.2. Analytical Methods

Six samples (1 pumice [Goodwill] and 5 lava [Diablotins, Micotrin, Grand Soufriere Hills, Plat Pays—Mt. Lofty, and Foundland]) were analyzed for whole-rock U-series isotopes at Macquarie University following the protocol described in *Heyworth et al.* [2007]. These data were collected in order to constrain zircon U-Th model ages. Analyses were obtained on a Nu Instruments® multicollector, inductively coupled plasma mass spectrometer using the $^{238}U/^{235}U$ ratio to determine the mass bias, assuming $^{238}U/^{235}U = 137.88$. Two measurements of TML-3 standard yielded activity ratios of $(^{230}Th)/(^{232}Th) = 1.067 \pm 0.006$ and $(^{238}U)/(^{232}Th) = 1.071 \pm 0.001$ (activities denoted by parentheses).

U-Th and U-Pb analyses of nonpolished crystal rims were performed on the UCLA CAMECA ims1270 secondary ion mass spectrometer following the method of *Schmitt et al.* [2010a]. Zircons with adhering glass were etched in 50% HF for 1–3 min. Zircons >30 μm in width were embedded in indium mounts; those <30 μm were embedded in high-purity aluminum. Analyses were undertaken in both mono and multicollector mode. For the monocollection session, secular equilibrium standard zircon AS3 yielded $(^{230}Th)/(^{238}U) = 1.013 \pm 0.008$ (mean square of weighted deviates MSWD = 2.8; n = 21), and for multicollection analyses the weighted average was 0.991 ± 0.005 (MSWD = 1.6; n = 23). Both data sets for AS3 are within uncertainty of the expected $(^{230}Th)/(^{238}U)$ secular equilibrium value of unity. Zircon crystallization ages were calculated using the two-point isochron method and the whole-rock $(^{230}Th)/(^{232}Th)$ and $(^{238}U)/(^{232}Th)$ ratios. Secular equilibrium grains (i.e., grains >350 ka that plotted on the equiline) were reanalyzed by U-Pb techniques. Relative sensitivities for Pb and U were determined on reference zircon AS3 [*Paces and Miller*, 1993]. Corrections for common Pb and ^{230}Th disequilibrium were applied following *Schmitt et al.* [2003].

For combined U-Th and (U-Th)/He analysis, zircon grains were extracted from the U-Th mounts, photographed, and packed into platinum tubes [*Schmitt et al.*, 2006]. Many of the zircons had low U concentrations (<100 ppm). For this reason, zircon with similar crystallization ages and from a single sample were, in some cases, packed into a single He aliquot. He degassing and isotope dilution ICP-MS analysis of U and Th were performed at the University of Texas at Austin following methods described in *Biswas et al.* [2007]. The alpha-ejection correction (Ft) factor was calculated using Monte-Carlo modeling following *Farley* [2002]. Zircon (U-Th)/He ages from the Fish Canyon Tuff standard average 27.8 ± 0.8 (RSD% 7.5; n = 162). Based on the reproducibility of Fish Canyon Tuff zircon standard data, we assigned an equivalent uncertainty (i.e., 8% at 1σ) to the individual (U-Th)/He ages prior to disequilibrium correction. Due to common uranium series disequilibrium in young zircons, ages assuming equilibrium of intermediate daughters in the U decay chain often underestimate the eruption age [*Farley et al.*, 2002]. Disequilibrium corrections were applied using the UCLA MCHeCalc program described in *Schmitt et al.* [2010b]. We report the individual disequilibrium-corrected ages, and a Gaussian fit for the average eruption age. Q values were used to quantify the goodness of fit as described by *Press et al.* [1992]. The average age was considered acceptable for Q > 0.01 and n ≥ 4, where n is the number of aliquots included in the sample set. Because all U-Th analyses on zircon are rim analyses, crystallization ages represent the lower limit of the bulk crystallization age. If crystals are highly zoned, the assumption of rim age as bulk age will lead to an overcorrected eruption age (i.e., the age will be too old, whereby the minimum age is constrained by that for secular equilibrium of the bulk crystal). Low Q values and eruption ages greater than U-Th crystallization ages provided indications of overcorrected values. In these cases, we assumed secular equilibrium for the crystal interior. In cases where the U-Th crystallization age was not determined, we assigned the average U-Th age of the selected sample to the zircon. In cases with multiple grains, the average U-Th ages of the grains was assigned to the aliquot. Grains <5 μg are considered the lower size limit of the technique, and those grains were omitted due to their high analytical uncertainties

3. Results

3.1. Eruption Ages From Combined U-Th and (U-Th)/He Zircon Geochronology

U-series isotopes from whole-rock samples were used to determine the two-point isochrons from which zircon U-Th crystallization ages are calculated. All samples yielded $(^{234}U)/(^{238}U)$ within error of unity (supporting information Table S1) indicating that the U-Th isotope concentrations have not been affected by secondary alteration. An exception is the Diablotins sample which has a 3% excess in ^{234}U over ^{238}U

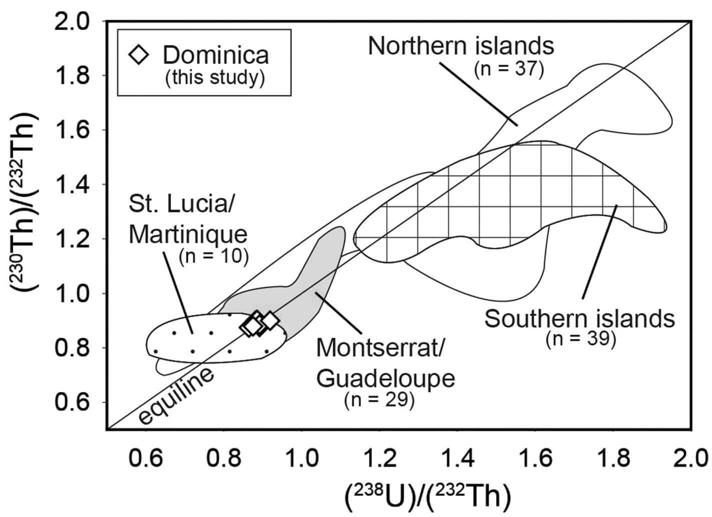

Figure 2. Whole rock U-series data for Dominica volcanic rocks. Values from other islands in the Lesser Antilles arc are shown for reference [*Turner et al*., 1996; *Heath et al*., 1998; *Chabaux et al*., 1999; *Zellmer et al*., 2003; *Toothill et al*., 2007; *DuFrane et al*., 2009; *Huang et al*., 2011].

activities and was omitted from isochron calculations. On a (^{238}U)/(^{232}Th) versus (^{230}Th)/(^{232}Th) equiline diagram, all samples plot within error of the equiline and have (^{230}Th)/(^{238}U) ratios ranging between 0.99 and 1.03 (corresponding to a mass ratio of U/Th of ~0.3; Figure 2).

Twelve eruption ages were determined using combined U-Th and (U-Th)/He zircon geochronology (Table 2, supporting information Table S2, and Figure 1). These ages range from 170 ± 14 to 8.1 ± 0.7 ka, with a single age of ~770 ka (Table 2, supporting information Table S2, and Figure 1). To cover a large number of samples, the number of replicates for each sample was necessarily limited (n = 3–11), but Q values are all >0.1 suggesting homogeneous age populations. Of the 10 centers dated by (U-Th)/He in this study, seven have been previously dated by other methods (Table 1). This permits some comparison, with the caveat that old K-Ar ages may be attributed to excess argon, which has been noted for multiple samples from the island [*Demange et al*., 1985; *Samper et al*., 2008]. Another problem is that many radiocarbon ages are near the limits of detection of ^{14}C and therefore should be considered as minimum ages (Table 1). The oldest center, Morne Espagnol, was previously dated at 2.2 ± 0.3 Ma by K-Ar (M. C. Monjaret, unpublished thesis, 1985), but produced a significantly younger (U-Th)/He age of 770 ± 46 ka (Table 2). The (U-Th)/He age of Aux Diables (170 ± 14 ka) is much older than published ^{14}C ages from its western flank and summit areas (>47 and ~44 ka; Table 1). Diablotins produced a (U-Th)/He age of 75 ± 4 ka with corresponding K-Ar and ^{14}C ages of 0.7 Ma to >47 ka, respectively. The (U-Th)/He age of Trois Piton (26 ± 3 ka), overlaps within error of previously published ^{14}C ages (28–18 ka; Table 1).^{14}C ages from Grand Soufrière Hills are concordant with the (U-Th)/He age of ~8 ka. The La Falaise

Table 2. Summary of (U-Th)/He Results[a]

Location No.	Unit	(U-Th)/He Age (ka)	N	Q
Northern Domes				
34	Aux Diables	170 (+14, −14)	4	0.287
37	Espagnol	744 (+46, −45)	7	0.766
41	Diablotins	75 (+4, −4)	8	0.336
Central Domes				
10	Micotrin	b.d.		
13	Trois Piton	26 (+2, −3)	4	0.169
29	Grand Soufriere Hills	8.1 (+0.7, −0.6)	5	0.0268
Morne Plat Pays				
19	Plat Pays [DM]	61 (+3, −3)	10	0.285
40	Plat Pays [L]	11 (+1, −1)	6	0.408
21	La Falaise	84 (+4, −5)	11	0.988
38	Fous	40 (+3, −3)	7	0.423
PPVC Domes				
24	Northern Rouge	9.9 (+0.7, −0.6)	6	0.408
25	Patates	b.d.		
26	Crabier	16 (+1, −1)	6	0.260
39	Southern Rouge	3.8 (+0.3, −0.3)	4	0.231

[a]N refers to the number of aliquots used to calculate the final age. Q represents the goodness-of-fit value. All ages shown are the average-corrected ages calculated using MCHeCalc. Errors shown are 1σ errors. b.d. = helium was below the detection limit and a (U-Th)/He age could not be calculated. For full aliquot data and details of the disequilibrium correction process, see supporting information Table S2.

deposit yielded a (U-Th)/He age of 84 ± 4 ka, close to the K-Ar age of ~96 ka [*Samper et al*., 2008]. The Morne Plat Pays [DM and L] samples yielded (U-Th)/He ages of 11 ± 1 and 61 ± 3 ka, respectively, which are older than the previously determined ^{14}C ages of ~6.6 ka for Morne Plat Pays at the Geneva Quarry location (Table 1). Because the DM and L samples for Morne Plat Pays studied here were collected at the edge of the depression margin (Location 19) and near the volcano's summit (Location 40), respectively, we suggest that these samples represent two different eruption events from this center that cannot be correlated to dated deposits previously ascribed to Morne Plat Pays [*Le Friant et al*., 2002; *Lindsay et al*., 2003]. (U-Th)/He ages for Micotrin and Patates are close to the detection limits and thus very imprecise due to extremely low He abundance, which suggests that these units are very young. This is consistent with the previous ^{14}C determinations of ~1100 and ~400–650 years, respectively (Table 1).

3.2. U-Th Zircon Rim Crystallization Ages

U-Th ages were determined on unpolished crystal faces and are interpreted to represent the final stages of zircon growth for individual crystals. Many of the samples from the domes deposits (i.e., Aux Diables, Diablotins, Trois Piton, Micotrin, Plat Pays [DM], Fous, and Patates) display zircon rim age distributions that range from the time of eruption indicated by the (U-Th)/He ages to secular equilibrium (>350 ka; Figures 3 and 4 and supporting information Table S3). In contrast, zircon crystal rims in Plat Pays [L], Crabier, and Rouge samples are all <50 ka in age (Figure 4 and supporting information Table S3). In most samples, the youngest crystal rim U-Th ages overlap within uncertainty of the (U-Th)/He eruption ages (Figures 3 and 4), supporting the robustness of this combined dating technique. Although zircon crystallization for the Morne Fous and Grand Soufrière Hills samples appears to have terminated ~10–20 ka prior to eruption, near-eruption rims may not have been preserved. Also, as the number of dated zircon crystals for these two samples is small (<15 rim analyses), it is possible that younger zircon crystallization may have gone undetected. Zircons from Diablotins differ from other Dominica samples in that the major U-Th crystallization peak and the (U-Th)/He eruption ages are indistinguishable. This suggests minor pre-eruptive residence of zircon beneath this center. In one case (Plat Pays [DM]), a substantial number of zircon rim ages are significantly younger than the associated (U-Th)/He age (Figure 4). The causes for this are not understood, in particular as replicate U-Th and (U-Th)/He analyses appear internally consistent. Because of this discrepancy, we consider the (U-Th)/He age of 61 ka as a maximum age for the eruption and suggest that the eruption age postdates ~20 ka, which is the youngest U-Th age determined for that deposit. In this case, the U-Th crystallization ages are considered more reliable than the (U-Th)/He ages because both the alpha-ejection correction and the disequilibrium corrections might have led to an overestimation of the eruption age [*Farley*, 2002; *Farley et al*., 2002]. Diablotins and Crabier have U-Th ages younger than the related eruption age at 1σ error levels, but because crystallization and eruption ages overlap at 2σ error, both ages are considered mutually supportive within stated uncertainties.

Probability density functions (PDF) of zircon age distributions from the lava dome samples are generally unimodal, with major crystallization peaks occurring within ~60 ka of the respective eruption (Figures 3 and 4). By contrast, zircon age distributions for all pyroclastic flow deposits display polymodal age distributions with ages ranging from the time of eruption to secular equilibrium (Figure 5 and supporting information Table S3). Several samples display overlapping peak ages in PDF curves at sufficiently high probabilities ($p > 0.05$) to accept the hypothesis that they sample the same age distributions based on Kolmogorov-Smirnov (KS) statistical analysis (Figure 6; see *Fletcher et al*. [2007] for method). Zircon crystallization ages in the Northern and Southern Rouge, Crabier, Plat Pays [L], and Micotrin samples all peak at ~15 ka with high KS probabilities (p ranging from 0.4 to ~1; Figure 6a). A second U-Th age group of zircons comprises the Plat Pays [DM], Trois Piton, and Grand Soufrière Hills samples which have overlapping peaks at ~45 ka with p values near unity (Figure 6b). Zircon U-Th ages in the La Falaise, Fous, and Diablotins samples display peaks at ~100 ka; their age distributions are also very similar with p ranging between 0.4 and ~1 despite the fact that they are geographically separated (Figure 6c). The oldest and northernmost sample, Aux Diables, has an apparent unimodal zircon crystallization peak at ~225 ka, but the high uncertainties of U-Th ages near secular equilibrium could mask any minor age variations. Regardless, this age is distinct from any of the other samples, as is the U-Pb age for the Espagnol Dome. The most recent dome, Patates, shows a minor young (<10 ka) zircon peak, similar to the peak in the other PPVC domes, but also has a second peak at ~30 ka. This combination of ages distinguishes Patates from the other domes, with low probabilities of similarity $p < 0.1$.

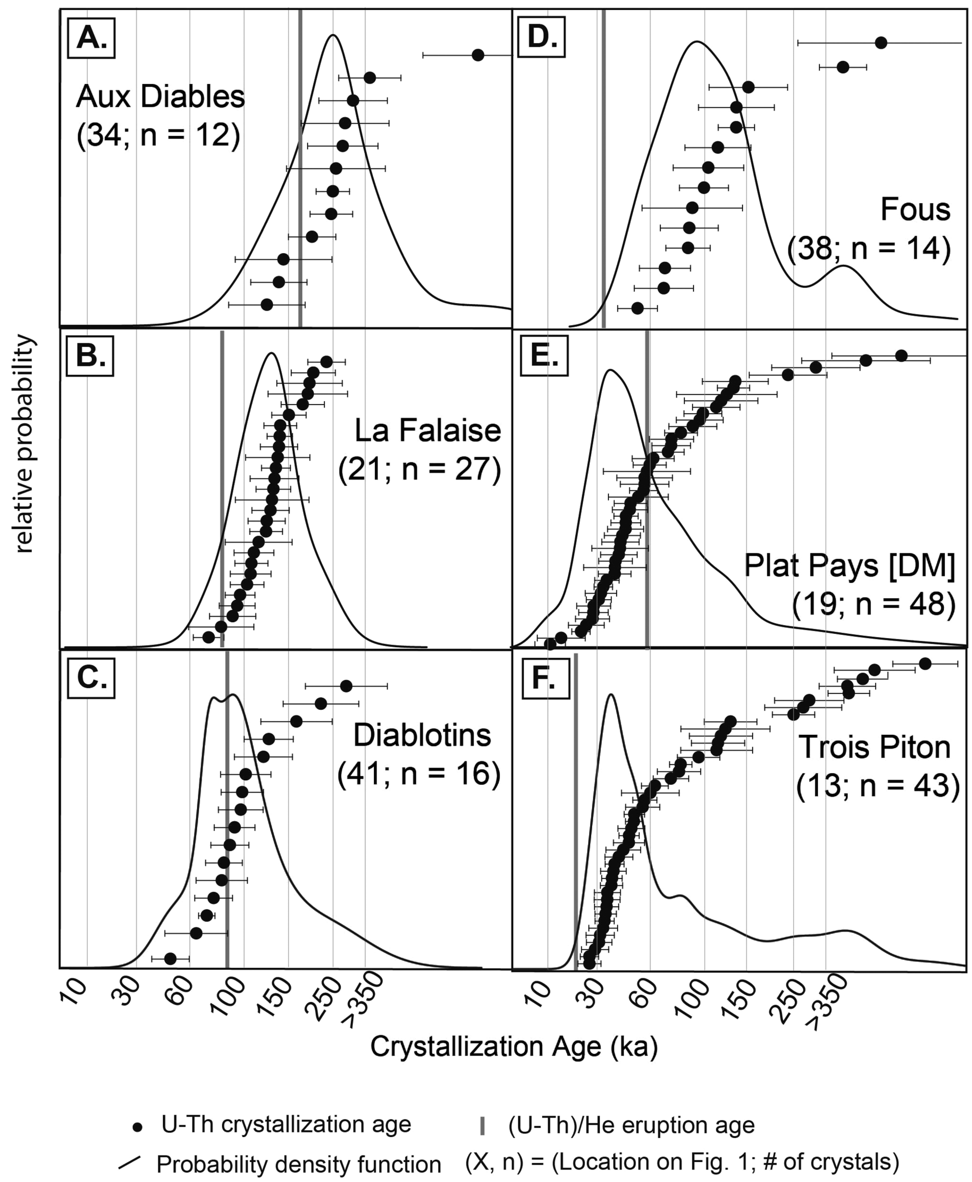

Figure 3. Rank-order plots and probability density distributions of U-Th zircon model ages for lava dome deposits with >20 ka eruption ages based on (U-Th)/He zircon geochronology. Ages are derived from two-point isochrons anchored using the whole-rock U-series values (see supporting information Table S2). Thick vertical lines indicate (U-Th)/He eruption age. Samples are organized according to eruption age from oldest to youngest.

In contrast to the domes, zircon spectra from all ignimbrites record multiple crystallization events (Figure 5). Within the ignimbrites, the three samples from the Roseau sequence (i.e., Goodwill Quarry, Link Flow 1, and Link Flow 3) have similar zircon age distributions with overlapping peaks at ~50 and ~100 ka ($p > 0.9$; Figures 6d and 6h). Layou and Londonderry display a different age distribution from the Roseau sequence ($p < 0.05$), but overlap with each other ($p =$ nearly 1; Figures 6d and 6h).

Based on the similarities in zircon age PDF curves (using KS statistics), zircons found in Dominica lava domes can be grouped into four categories which record diachronous phases of zircon crystallization occurring at ~250 ka (Group 1), ~100 (Group 2), ~45 (Group 3), and ~10 ka (Group 4) (Figure 7). The corresponding range of eruption ages of these phases are ~170, 40–84, 8–26, and 4–16 ka, respectively. In many cases, eruption centers which display overlapping zircon crystallization peaks are up to 40 km apart in map view (Figure 7g) and have eruption ages that differ by up to ~40 ka. While zircons in the ignimbrites preserve

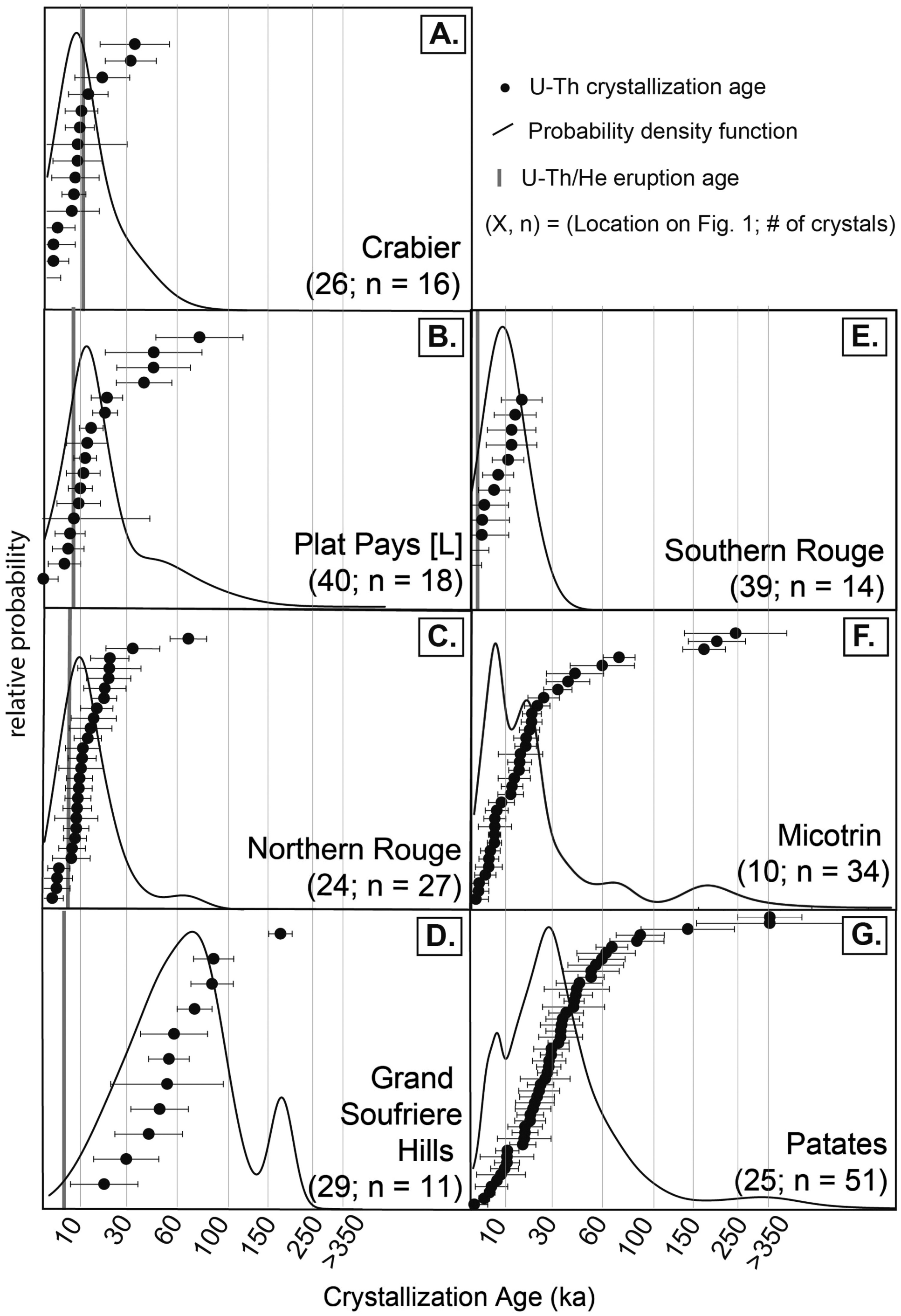

Figure 4. Rank-order plots and probability density distributions of U-Th zircon model ages for lava dome deposits with <20 ka eruption ages based on (U-Th)/He zircon geochronology. See caption Figure 3 for details on age calculation and presentation.

multiple crystallization events, peaks within zircon age spectra for these deposits overlap with those present in the lava domes (Figure 7f).

3.3. U-Pb Zircon Ages

Crystals with secular equilibrium U-Th ages were identified in nine samples and reanalyzed by U-Pb techniques (supporting information Table S4 and Figure 8). These analyses are reconnaissance because

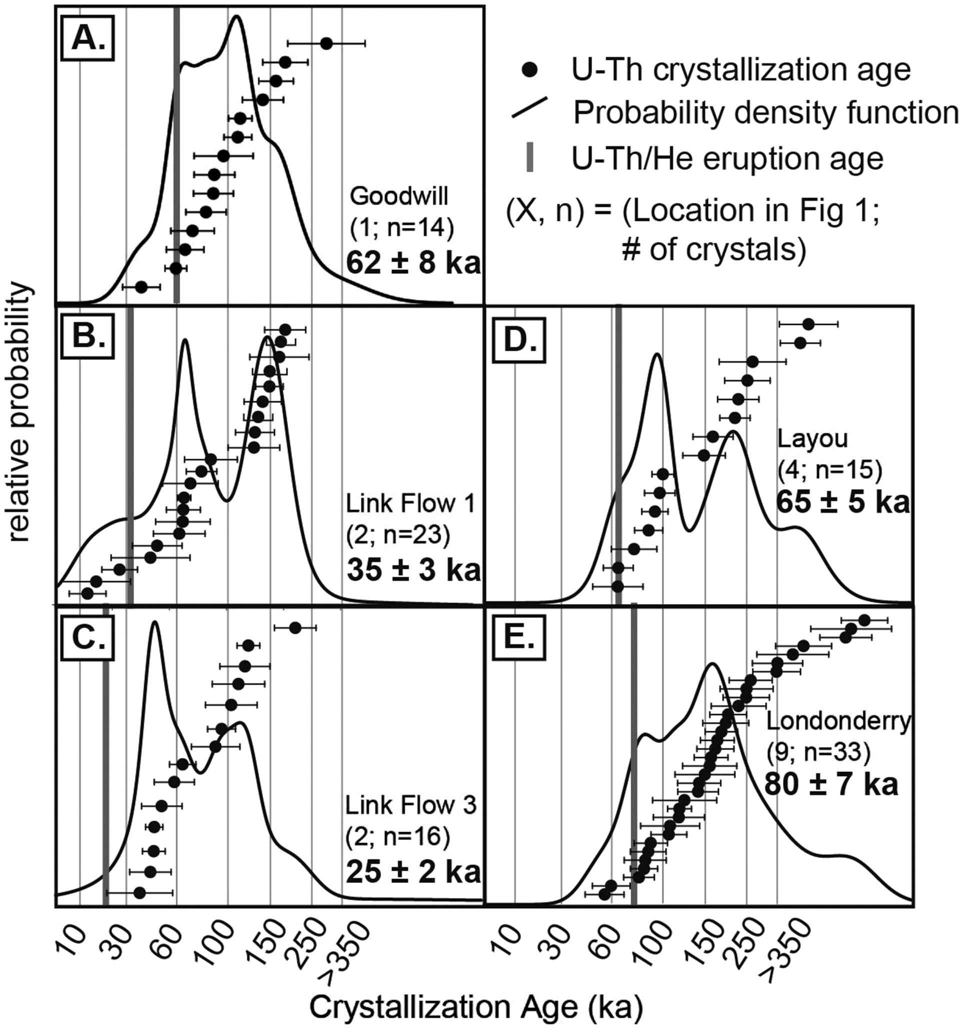

Figure 5. Rank-order plots and probability density distributions of U-Th zircon model ages for pumiceous pyroclastic flow deposits. Thick vertical lines indicate (U-Th)/He eruption age from *Howe et al.* [2014].

rims were affected by high common Pb which limits precision for individual ages. This was further confounded by low U and the young ages (frequently near the secular-equilibrium limit of U-Th geochronology of ~350 ka) of most of the crystals. Of the 50 crystals analyzed, only nine yielded ages >1 Ma. Although the majority of the older crystals in Aux Diables, Patates, and Espagnol domes have ages between ~1 and 2 Ma, there are a few pre-Quaternary crystals (between 6.4 ± 2.2 and 54 ± 19 Ma) in the Aux Diables sample (Figure 8). Secular equilibrium zircons from Plat Pays, Trois Piton, Micotrin, Fous, and Londonderry all yielded ages <1 Ma.

3.4. Zircon U and Th Abundances and Saturation Temperatures

Uranium abundances in zircon are mostly in the range of ~25–350 ppm (average = 150 ± 20 ppm). Crystals with U concentrations >350 ppm are rare. Thorium concentrations range from ~10 to 500 ppm (average = 70 ± 40) with Th/U (average= 0.47 ± 0.1) typical for magmatic zircon [*Hoskin and Schaltegger*, 2003]. There are no clear trends between crystallization age and Th or U composition. Based on a simple mass balance calculation (assuming that U is entirely partitioned into the melt phase), average whole-rock U abundances of ~1 ppm translate into 1.5 and 2 ppm melt U at crystal abundances of 35% for the pumices and 50% for the lava dome samples, using modal crystal abundances. These melt U abundances are broadly consistent with the average zircon U abundance and a typical zircon-melt partitioning coefficient D = 100 [*Blundy and Wood*, 2003].

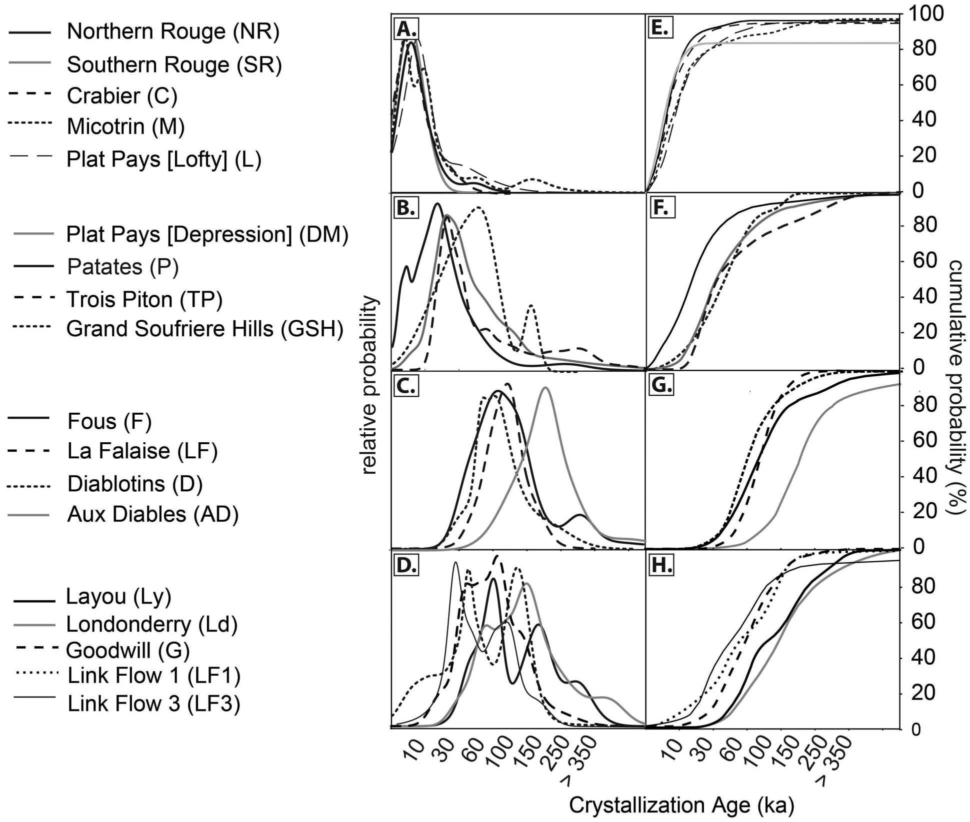

I.	SR	C	M	L
NR	0.5	0.9	0.9	0.8
SR		1.0	0.4	0.9
C			0.9	1.0
M				1.0

J.	DM	TP	GSH
P	0	0	0
DM		1.0	1.0
TP			1.0

K.	F	LF	D
AD	0	0	0
F		1.0	0.9
LF			0.4

L.	Ld	G	LF1	LF3
Ly	1.0	0.5	0.2	0.2
Ld		0	0	0
G			1.0	0.9
LF1				1.0

Figure 6. (a–h) Zircon crystallization age probability density curves showing results of Kolmogorov-Smirnov (KS) statistical comparison between age populations. (i–l) Boxes show probabilities between individual units. Probabilities $p > 0.05$ indicate that the populations being compared are indistinguishable at the 95% confidence level [*Press et al*., 1992]. Dark gray boxes have correlations >0.05. White boxes have $p < 0.05$. Samples are abbreviated as shown next to the sample names.

Zircon saturation temperatures calculated using whole-rock compositions and calibrations in *Watson and Harrison* [1983] and *Boehnke et al*. [2013] range from 695 to 748°C and from 629 to 698°C, respectively. However, Dominica rocks contain abundant phenocrysts (~50%) so that glass compositions are more representative for the melt than whole-rock compositions and are consequently better suited to calculate realistic zircon saturation temperatures [e.g., *Harrison et al*., 2007]. Using the same mass balance calculation as above (no Zr partitioning into major phases), the estimated Zr in the melt is 170 and 303 ppm for pumices and lava dome samples, respectively. Using these values and the glass compositions analyzed by electron microprobe for Dominica rocks [*Halama et al*., 2006; *Howe et al*., 2014] increases the corresponding range in zircon saturation temperatures to 720–840°C. These values are maximum values because some Zr will be sequestered in the major phases, but because of low partitioning values for Zr in these phases, it is reasonable to assume this only represents a small fraction of the bulk Zr abundance of the rocks. The zircon saturation temperatures for Dominica rocks are thus in the lower range of the near-eruption temperatures determined by Fe-Ti oxide thermometry which are ~800–880°C for PPVC [*Halama et al*., 2006] and ~750–900°C for other Dominica magmas [*Howe et al*., 2014].

4. Discussion

4.1. Zircon Saturation Thermometry: Evidence for Zircon Provenance From Differentiated Melt Pockets

Zircon crystallization is controlled by the Zr concentration of the melt, temperature, and the melt major element composition [*Watson and Harrison*, 1983; *Boehnke et al*., 2013]. Because the zircon saturation temperatures determined using glass compositions overlap with the pre-eruptive magmatic temperatures (section 3.5), it is likely that zircon found within the andesitic deposits crystallized in a fractionated melt that was equally or even more evolved than the interstitial glass of Dominica pumice or lava. This implies either the

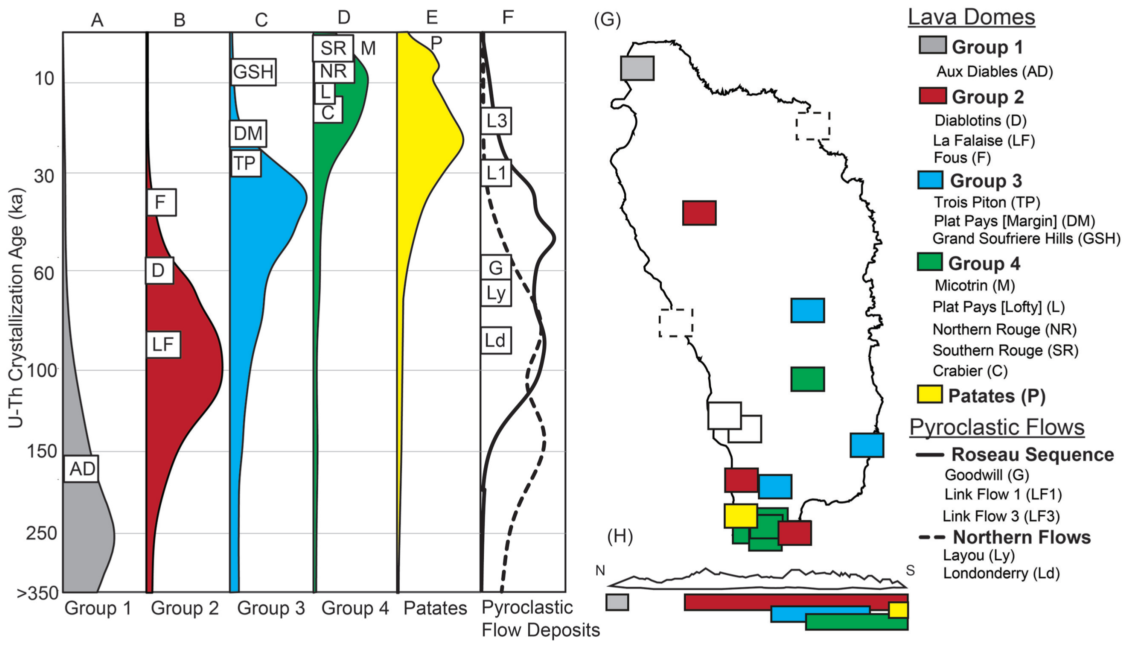

Figure 7. Summary of U-Th zircon rim crystallization ages. (a–d) Crystallization peaks of the lava dome deposits. Samples are grouped based on overlapping KS statistics, which show correlation of zircon populations (see Figure 6). (e) Crystallization peaks of Patates; note that Patates displays a separate crystallization peak from other domes. (f) Crystallization history of pyroclastic flow deposits. Lettered boxes represent eruption ages based on (U-Th)/He zircon geochronology. Eruption ages from Micotrin (M) and Patates (P) are from ^{14}C ages (see Table 1). (g) Geographic distribution of samples belonging to each crystallization group. (h) Schematic cross section of island showing possible range of magmatic correlation for different crystallization phases. This cross section illustrates distance only and does not imply variation of depth between groupings. Note: Morne Espagnol is not included in this figure as all of its zircons are older than the limit of U-Th analysis (~350 ka).

presence of a highly silicic reservoir, such as was suggested by *Halama et al*. [2006] for the PPVC, or the existence of differentiated melts pockets within a highly crystalline reservoir of intermediate bulk composition. In either case, the erupted magmas of intermediate composition are produced by magma mixing and/or thermal rejuvenation of evolved magma reservoirs [e.g., *Kent et al*., 2010]. The presence of zircons in all domes implies that such highly differentiated melts were associated with each of the centers, and thus their presence can be inferred over much of the island.

4.2. Significance of Zircon Rim Ages: Crystal Recycling and the Presence of Crystal-Mush

Based on direct dating of individual crystals, *Miller et al*. [2007] proposed three zircon categories: (1) zircon crystallized from the accompanying melt phase (autocrysts); (2) zircon recycled from earlier magmatic events (antecrysts), and (3) zircon entrained from surrounding country rock (xenocrysts). It is recognized that often complex growth relations exist in individual crystals that blur the limits between these categories. Few studies have specifically targeted the unpolished rims of zircon crystals [*Reid and Coath*, 2000; *Bindeman et al*., 2006; *Storm et al*., 2012]. Where rims of separate crystals in the same hand specimen reveal age differences of up to several hundred thousand years, they provide evidence that the crystals experienced distinct thermal histories [*Miller and Wooden*, 2004; *Claiborne et al*., 2010b; *Storm et al*., 2012]. In the case of Dominica, most samples display a wide range of zircon rim ages extending from the time of eruption to secular equilibrium (~350 ka; Figures 3–5), with many samples showing near continuous crystallization throughout their magmatic history.

The large spread in individual zircons age spectra for Diablotins, Trois Piton, Micotrin, and Morne Plat Pays (from eruption to secular equilibrium; Figures (3 and 4)) indicates that the zircon crystals were in contact with melt at varying times and were subsequently mixed back together just prior to eruption. The lack of resorbed zircon crystal faces is inconsistent with prolonged contact with a zircon-undersaturated melt, and the presence of older rim ages implies that crystals were intermittently out of contact with the melt phase. Such separation could be the result of storage in a subsolidus part of the magma reservoir or as inclusions in phenocryst phases (as discussed by *Storm et al*. [2012]). However, because the analyzed zircons typically had adherent glass, we favor the interpretation that zircons

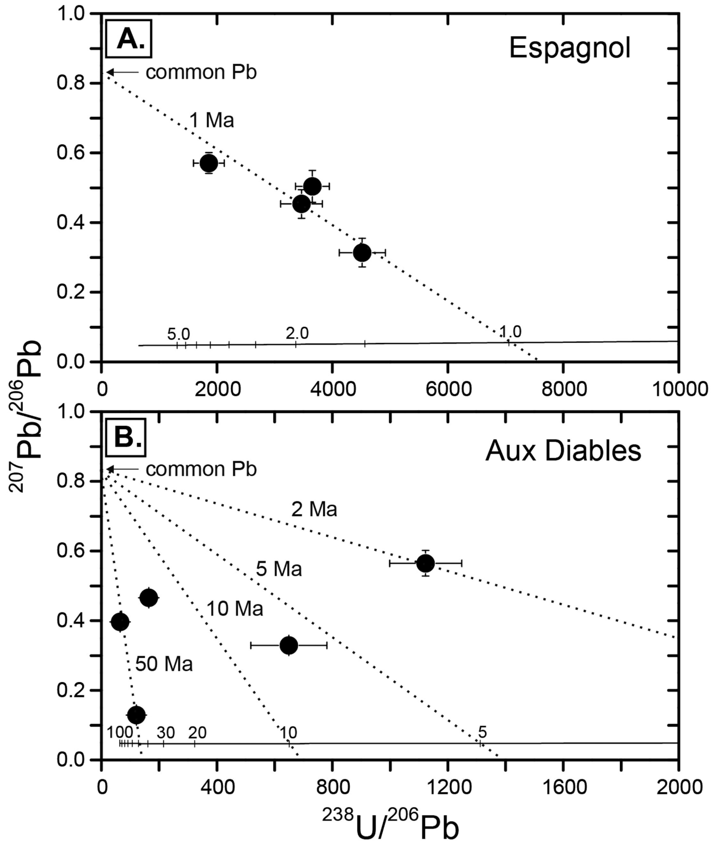

Figure 8. U-Pb zircon analyses for (a) Aux Diables and (b) Morne Espagnol uncorrected for common Pb. Mixing lines between radiogenic U/Pb and common Pb (with $^{207}Pb/^{206}Pb = 0.83$, typical for Southern California anthropogenic Pb as a surface contaminant [*Sañudo-Wilhelmy and Flegal*, 1994]) are indicated with their corresponding concordia intercept ages. For clarity, analyses with <30% radiogenic are omitted.

initially crystallized in evolved interstitial melt pockets associated with highly crystalline crystal mushes of intermediate (andesitic) bulk composition, and were then recycled back into the erupted melt via "defrosting" [*Mahood*, 1990] of the crystalline framework. Crystal recycling from mushy or subsolidus intrusions has also been invoked at other intra-oceanic arc settings based on evidence for mixed crystal populations and frequent disequilibrium between crystals and host melt [e.g., *Barker et al*., 2012]. The presence of rim ages that overlap within error of the (U-Th)/He age suggests that crystallization, and hence melt presence under conditions of zircon saturation, continued to occur at least in some parts of the intrusive complex up to the time of eruption. The preservation of older rim ages thus also implies that liberation from any subsolidus portions of the magma chamber and subsequent ascent likely occurred relatively rapidly, i.e., at a rate faster than the time necessary to grow or resorb a measurable rim thickness.

In contrast, several of the younger lava samples (e.g., Plat Pays [L], northern and southern Rouge, and Crabier) have exclusively young zircon rim ages (<50 ka; Figure 4). Several processes are possible to explain this: (1) the magmatic reservoir beneath these centers only recently became active; (2) the most recent period of zircon crystallization resulted in ubiquitous overgrowth on relic crystals; (3) the population of relic crystals was swamped by new crystals; and/or (4) preexisting crystals were obliterated at some point prior to ~50 ka. To distinguish between these scenarios would require age information from zircon cores which were not acquired in this study. Regardless, the zircon rim age spectra for Plat Pays [L], northern and southern Rouge, and Crabier that are distinct from Patates reveal that different zircon histories are recorded within closely spaced volcanic centers, less than 5 km apart.

KS analysis of zircon ages in pyroclastic deposits (Figure 6) identifies two groups: (1) the southern ignimbrites (e.g., Roseau Tuff, Link Flow 1, and Link Flow 2) and (2) Layou and Londonderry ignimbrites (Figure 7f). These groupings are supported by whole-rock, glass, and mineral geochemistry, which suggest that the southern ignimbrites are all related to a single source [*Howe et al*., 2014]. The putative sources are Wotten Waven/Micotrin dome for the southern ignimbrites and Trois Piton dome for the Layou ignimbrite [*Smith et al*., 2013]. Although peaks within the zircon age spectra from the ignimbrites overlap with peaks present in the lava dome samples (Figure 7), suggesting they share a common source, the ignimbrites display a greater abundance of antecrystic zircons. A direct comparison is complicated by uncertainties in the sources of ignimbrites and the different eruption ages, but we speculate that large-volume pyroclastic eruptions are more disruptive in their magma storage reservoirs compared to dome-forming eruptions, and thus sample larger and more age-heterogeneous parts of these reservoirs.

4.3. Genesis of an Island-Wide Silicic Intrusive Complex Beneath Dominica

Based on homogenous whole-rock compositions from volcanoes across the island and heterogeneous mineral chemistry seen in individual lava samples, *Smith et al*. [2013] proposed that Dominica is underlain by a large-scale mid-crustal intrusive complex which formed via the amalgamation of smaller magmatic chambers associated with individual volcanoes. The incremental growth of plutons by accumulation of small magmatic additions is a model developed for batholith-scale intrusions in continental arcs [*Glazner et al*., 2004; *de Silva and Gosnold*, 2007; *Claiborne et al*., 2010a]. On Dominica, protracted zircon age spectra (Figure 7h) imply that individual domes tap a periodically reactivated crystal mush zone, which may span the length of the island.

Combining PDF curves of zircon ages from individual volcanic rocks provides a first-order graphical representation about the durations and potential episodicity of crystallization within the reservoir feeding volcanic eruptions [*Lowenstern et al*., 2000; *Bacon and Lowenstern*, 2005; *Charlier et al*., 2005]. The U-Th zircon ages presented here are indicative of the timing of crystallization in the magma and represent the final episode of zircon growth experienced by the crystal prior to eruption. Thus, the age peaks in PDF curves can be interpreted as the terminal crystallization episodes experienced by major populations of crystals prior to eruption. Heterogeneity of rim ages underscores that individual zircon crystals can record crystallization events in parts of the subterraneous magmatic system which may be isolated from each other. The cumulative zircon age PDF curve of a sample, however, has been demonstrated to reveal characteristic patterns of zircon crystallization that can fingerprint individual magmatic centers [e.g., *Schmitt et al*., 2010b]. Moreover, sequentially erupted lavas tapping the same magma system can result in systematic relations between zircon rims and interiors that stem from progressive crystallization and/or zircon recycling in individual magmatic reservoirs [e.g., *Storm et al*., 2012]. This is the basis of using PDF curves to relate spatially separated volcanic rocks to a common magmatic source and to track the evolution of the magma system at depth.

Based on the KS statistics, PDF curves from Dominica lava domes fall into four separate possible magmatic groupings (Figure 7), which in some cases comprise domes that are up to 40 km apart on the surface. This suggests that zircon crystallization records widespread, episodic thermal rejuvenation. The spatial relationship between the magmatic groups also indicates a progressive movement of crystallization from north to south (at least for the dome samples; Figures 7g and 7h). This suggests that the magmatic foci leading to construction of the intracrustal magma reservoirs migrated arc-parallel with time. Such arc-parallel movement has been suggested for several islands in the Lesser Antilles, including Montserrat, St. Kitts, Guadeloupe, and St. Vincent, and has been attributed to changes in the orientation of downgoing slab due to the growth of the accretionary prism [*Harford et al*., 2002].

Three centers deserve special discussion: Aux Diables, Morne Espagnol, and the PPVC. Aux Diables is older than the other centers, with many of its zircons at or near secular equilibrium, and as the only tholeiitic center on the island has a strikingly different geochemical composition [*Smith et al*., 2013]. Based on this, we concur with *Smith et al*. [2013] that Aux Diables is likely magmatically separate from other centers on the island. Morne Espagnol, also in the North, is exceptional because of its comparatively old zircon ages ($\sim$1 Ma; Figure 8). In contrast, the majority of PPVC centers in the south display exclusively young rim ages, suggesting that this region may be the site of new magma injection and reservoir growth. Based on the high crystallinities of PPVC lava samples, which contain large crystals indicative of an extensive cooling period, and low Fe-Ti oxide temperatures, *Halama et al*. [2006] suggested that the PPVC lava domes sit atop a long-lived, shallow magma reservoir, which has been active for $>$100 ka. This scenario agrees broadly with our zircon spectra for Patates, but not with zircon spectra from Crabier and Rouge, despite all domes being similar in composition and crystallinity. However, as our data consist only of rim ages, it is possible that older zircons were overgrown or obliterated which could underestimate the longevity of the reservoir tapped by Crabier and Rouge.

Based on nearly continuous zircon crystallization in spatially separated domes of Dominica, we can refine the *Smith et al*. [2013] model that a batholith has amalgamated beneath the central and southern parts of Dominica throughout the Pleistocene-Holocene, stretching from Diablotins to the southern tip of the island. The beginnings of this nearly island-wide intrusive complex remain obscure because our study concentrated on final zircon growth, but reconnaissance U-Pb zircon rim ages for the southern domes are exclusively $<$2 Ma implying that it is entirely Quaternary in age.

4.4. Implications of Ancient Zircons and Crustal Maturation in Intra-oceanic Arcs

Given the complexity of interpreting zircon age distributions, it is often difficult to determine comagmatic (autocrystic and antecrystic) from xenocrystic zircons which have been assimilated from a contaminant source. U-Pb ages for Dominica zircons range from ~400 to ~50 Ma. As volcanic activity on Dominica has been occurring since the late Miocene [~7 Ma; *Smith et al*., 2013], we suggest that only grains >7 Ma are xenocrystic sensu stricto (i.e., inherited from the overriding arc crust). The majority of zircons analyzed by U-Pb are <7 Ma old and are thus considered antecrysts liberated from subsolidus storage just prior to eruption (as they do not have a young zircon rim). The predominance of zircons <1–2 Ma in Dominica volcanic rocks suggests that silicic magmatism producing zircon crystals beneath the island is a relatively recent development.

Zircon xenocrysts provide evidence for crustal contamination in magmas [e.g., *Charlier et al*., 2010]. Such crystals have been found in ancient, uplifted arc sequences and been attributed to assimilation of material from the overriding crust [*Smyth et al*., 2007; *Bosch et al*., 2011]. Two Eocene zircons (from the Aux Diables sample) provide evidence for relic prearc basement beneath Dominica and could be related to Eocene arc volcanism [50–60 Ma; *Bouysse and Westercamp*, 1990; *Rao*, 2008]. Although crustal contamination has been invoked to explain trace element patterns and Sr-Nd-Pb isotopic compositions of volcanic rocks on St. Lucia [*Bezard et al*., 2014], the relic zircons in Dominica rocks represent the first tangible evidence that such ancient silicic crustal rocks exist beneath the modern arc.

Intra-oceanic arcs have been suggested as one of the primary locations for the generation of continental crust [e.g., *Taylor*, 1967; *Scholl and von Huene*, 2009]. Recent geophysical surveys of the Izu-Bonin [*Kodaira et al*., 2007; *Takahashi et al*., 2008] and Lesser Antilles [*Kopp et al*., 2011] arcs indicate they are partly underlain by thick layers (>10 km) of intermediate plutonic material with seismic velocities similar to continental crust. Geophysical surveys of the Aleutian arc, however, find no such intermediate layer [*Holbrook et al*., 1999; *Fliedner and Klemperer*, 2000]. This suggests that both Izu-Bonin and the Lesser Antilles are locally composed of "mature" overriding crust. However, the timescales and mechanisms associated with such maturation are poorly understood. Zircon data from Dominica suggests that extensive plutons connecting volcanoes at depth can be built over a period of 1–2 Ma. The zircon crystallization histories are similar to those seen in continental arcs, suggesting that preexisting continental crust is not necessary for rapidly constructing voluminous batholith-like silicic bodies in intra-oceanic arc settings.

5. Conclusions

The intra-oceanic arc volcanoes of Dominica have complex magmatic histories. Zircon U-Th ages suggest the presence of highly evolved melt beneath much of the island for the last 1–2 Ma. Overlapping peaks in zircon crystallization from deposits erupted from spatially separated vents (~40 km) point to the existence of a laterally continuous midcrustal intrusive complex beneath Dominica. Most eruption deposits display a wide zircon age distribution (>350 ka range), indicating the magmatic system comprises a long-lived, periodically reactivated mush-zone. Overall, there is a broad trend of "peak crystallization" that migrated south (arc-parallel) across the island. Notably, zircon crystallization age spectra from voluminous pyroclastic deposits are different from those of individual lava domes erupted within the putative vent regions of the pyroclastic deposits, pointing to as of now poorly understood complexities within the magma reservoirs that fed these eruptions. Some morphologically pristine lava domes of the PPVC display exclusively young zircon rim ages (<50 ka) with narrow crystallization peaks, suggesting the ongoing construction of a new magma reservoir beneath the southern portion of the island. Overall, the zircon data is consistent with the development of an island-wide plutonic complex that has rapidly evolved in the last 1–2 Ma. This indicates that the magmatic processes operating beneath Dominica are similar to those seen in continental arcs. Thus, we suggest that the magmatic system at Dominica is a modern example of crustal evolution and thickening via magmatic accumulation and differentiation that may ultimately could lead to the formation of continental crust.

Acknowledgments
Brian Jicha and Jorge Vazquez are thanked for constructive reviews. Roman Kislitsyn and Michael Turner are thanked for technical support. This study was funded by a University of Auckland Doctoral scholarship, an internal University of Auckland PBRF grant and a New Zealand GNS Science contract to P.S., and a New Zealand Earthquake Commission grant to J.M.L. The ion microprobe facility at UCLA is partly supported by a grant from the Instrumentation and Facilities Program, Division of Earth Sciences, National Science Foundation. All data used in this publication can be found in the supporting information.

References

Annen, C., J. D. Blundy, and R. S. J. Sparks (2006), The genesis of intermediate and silicic magmas in deep crustal hot zones, *J. Petrol.*, *47*, 505–539, doi:10.1093/petrology/egi084.

Bachmann, O., and G. W. Bergantz (2003), Rejuvenation of the Fish Canyon magma body: A window into the evolution of large-volume silicic magma systems, *Geology*, *31*(9), 789–792, doi:10.1130/G19764.1.

Bachmann, O., B. L. A. Charlier, and J. B. Lowenstern (2007), Zircon crystallization and recycling in the magma chamber of the rhyolitic Kos Plateau Tuff (Aegean arc), *Geology*, *35*(1), 73–76, doi:10.1130/G23151A.1.

Bacon, C. R., and J. B. Lowenstern (2005), Late Pleistocene granodiorite source for recycled zircon and phenocrysts in rhyodacite lava at Crater Lake, Oregon, *Earth Planet. Sci. Lett.*, *233*(3–4), 277–293, doi:10.1016/j.epsl.2005.02.012.

Barker, S. J., C. J. N. Wilson, J. A. Baker, M. A. Millet, M. D. Rotella, I. C. Wright, and R. J. Wysoczanski (2012), Geochemistry and petrogenesis of silicic magmas in the intra-oceanic Kermadec Arc, *J. Petrol.*, *54*(20), 351–391, doi:10.1093/petrology/egs07.

Bellon, H. (1988), Reconnaissance chronologique des deux premieres phases d'activite volcanique en Dominique (Petites Antilles), *C. R. Acad. Sci. Ser. II*, *306*, 1487–1492.

Bezard, R., J. P. Davidson, S. Turner, C. G. Macpherson, J. M. Lindsay, and A. J. Boyce (2014), Assimilation of sediments embedded in the oceanic arc crust: Myth or reality?, *Earth Planet. Sci. Lett.*, *395*, 51–60, doi:10.1016/j.epsl.2014.03.038.

Bindeman, I., A. Schmitt, and J. Valley (2006), U–Pb zircon geochronology of silicic tuffs from the Timber Mountain/Oasis Valley caldera complex, Nevada: Rapid generation of large volume magmas by shallow-level remelting, *Contrib. Mineral. Petrol.*, *152*(6), 649–665, doi:10.1007/s00410-006-0124-1.

Biswas, S., I. Coutand, D. Grujic, C. Hager, D. Stöckli, and B. Grasemann (2007), Exhumation and uplift of the Shillong plateau and its influence on the eastern Himalayas: New constraints from apatite and zircon (U-Th-[Sm])/He and apatite fission track analyses, *Tectonics*, *26*, TC6013, doi:10.1029/2007TC002125.

Blundy, J., and B. Wood (2003), Mineral-melt partitioning of uranium, thorium and their daughters, *Rev. Mineral. Geochem.*, *52*(1), 59–123, doi:10.2113/0520059.

Boehnke, P., E. B. Watson, D. Trail, T. M. Harrison, and A. K. Schmitt (2013), Zircon saturation re-revisited, *Chem. Geol.*, *351*, 324–334, doi:10.1016/j.chemgeo.2013.05.028.

Bosch, D., C. J. Garrido, O. Bruguier, B. Dhuime, J.-L. Bodinier, J. A. Padròn-Navarta, and B. Galland (2011), Building an island-arc crustal section: Time constraints from a LA-ICP-MS zircon study, *Earth Planet. Sci. Lett.*, *309*(3–4), 268–279, doi:10.1016/j.epsl.2011.07.016.

Bouysse, P., and D. Westercamp (1990), Subduction of Atlantic aseismic ridges and Late Cenozoic evolution of the Lesser Antilles island arc, *Tectonophysics*, *175*(4), 349–380, doi:10.1016/0040-1951(90)90180-G.

Boynton, C., G. Westbrook, M. Bott, and R. Long (1979), A seismic refraction investigation of crustal structure beneath the Lesser Antilles island arc, *Geophys. J. Int.*, *58*(2), 371–393, doi:10.1111/j.1365-246X.1979.tb01031.

Brophy, J. G. (2008), A study of rare earth element (REE)-SiO_2 variations in felsic liquids generated by basalt fractionation and amphibolite melting: A potential test for discriminating between the two, *Contrib. Mineral. Petrol.*, *156*, 337–357, doi:10.1007/s00410-008-0289-x.

Brown, G., J. Holland, H. Sigurdsson, J. Tomblin, and R. Arculus (1977), Geochemistry of the Lesser Antilles volcanic island arc, *Geochim. Cosmochim. Acta*, *41*(6), 785–801, doi:10.1016/0016-7037(77)90049-7.

Chabaux, F., C. Hémond, and C. J. Allègre (1999), ^{238}U–^{230}Th–^{226}Ra disequilibria in the Lesser Antilles arc: Implications for mantle metasomatism, *Chem. Geol.*, *153*(1–4), 171–185, doi:10.1016/S0009-2541(98)00160-0.

Charlier, B., D. W. Peate, C. J. Wilson, J. B. Lowenstern, M. Storey, and S. J. Brown (2003), Crystallisation ages in coeval silicic magma bodies: ^{238}U–^{230}Th disequilibrium evidence from the Rotoiti and Earthquake Flat eruption deposits, Taupo Volcanic Zone, New Zealand, *Earth Planet. Sci. Lett.*, *206*(3), 441–457, doi:10.1016/S0012-821X(02)01109-3.

Charlier, B., C. J. N. Wilson, J. B. Lowenstern, S. Blake, P. W. Van Calsteren, and J. P. Davidson (2005), Magma generation at a large, hyperactive silicic volcano (Taupo, New Zealand) revealed by U–Th and U–Pb systematics in zircons, *J. Petrol.*, *46*(1), 3–32, doi:10.1093/petrology/egh060.

Charlier, B., C. J. N. Wilson, and N. Mortimer (2010), Evidence from zircon U-Pb age spectra for crustal structure and felsic magma genesis at Taupo volcano, New Zealand, *Geology*, *38*(10), 915–918, doi:10.1130/G31123.1.

Christeson, G. L., P. Mann, A. Escalona, and T. J. Aitken (2008), Crustal structure of the Caribbean–northeastern South America arc-continent collision zone, *J. Geophys. Res.*, *113*, B08104, doi:10.1029/2007JB005373.

Claiborne, L. L., C. F. Miller, and J. L. Wooden (2010a), Trace element composition of igneous zircon: A thermal and compositional record of the accumulation and evolution of a large silicic batholith, Spirit Mountain, Nevada, *Contrib. Mineral. Petrol.*, *160*(4), 511–531, doi:10.1007/s00410-010-0491-5.

Claiborne, L. L., C. F. Miller, D. M. Flanagan, M. A. Clynne, and J. L. Wooden (2010b), Zircon reveals protracted magma storage and recycling beneath Mount St. Helens, *Geology*, *38*(11), 1011–1014, doi:10.1130/G31285.1.

Cooper, K. M., and A. J. Kent (2014), Rapid remobilization of magmatic crystals kept in cold storage, *Nature*, *506*, 480–483, doi:10.1038/nature12991.

Demange, J., H. Leborne, H. Traineau, and D. Westercamp (1985), Histoire volcano-structurale de la region sud de la Dominique, *Tech. Rep. 85 SGN 068 IRG-GTH*, Inst. Mixte de Rech. Geotherm., Orleans, France.

de Silva, S. L., and W. D. Gosnold (2007), Episodic construction of batholiths: Insights from the spatiotemporal development of an ignimbrite flare-up, *J. Volcanol. Geotherm. Res.*, *167*(1), 320–335, doi:10.1016/j.jvolgeores.2007.07.015.

DuFrane, S. A., S. Turner, A. Dosseto, and M. van Soest (2009), Reappraisal of fluid and sediment contributions to Lesser Antilles magmas, *Chem. Geol.*, *265*(3–4), 272–278, doi:10.1016/j.chemgeo.2009.03.030.

Farley, K. A. (2002), (U-Th)/He dating: Techniques, calibrations, and applications, *Rev. Mineral. Geochem.*, *47*(1), 819–844, doi:10.2138/rmg.2002.47.18.

Farley, K. A., B. P. Kohn, and B. Pillans (2002), The effects of secular disequilibrium on (U–Th)/He systematics and dating of Quaternary volcanic zircon and apatite, *Earth Planet. Sci. Lett.*, *201*(1), 117–125, doi:10.1016/S0012-821X(02)00659-3.

Fletcher, J. M., M. Grove, D. Kimbrough, O. Lovera, and G. E. Gehrels (2007), Ridge-trench interactions and the Neogene tectonic evolution of the Magdalena shelf and southern Gulf of California: Insights from detrital zircon U-Pb ages from the Magdalena fan and adjacent areas, *Geol. Soc. Am. Bull.*, *119*(11–12), 1313–1336, doi:10.1130/B26067.1.

Fliedner, M. M., and S. L. Klemperer (2000), Crustal structure transition from oceanic arc to continental arc, eastern Aleutian Islands and Alaska Peninsula, *Earth Planet. Sci. Lett.*, *179*(3–4), 567–579, doi:10.1016/S0012-821X(00)00142-4.

Glazner, A. F., J. M. Bartley, D. S. Coleman, W. Gray, and R. Z. Taylor (2004), Are plutons assembled over millions of years by amalgamation from small magma chambers?, *GSA Today*, *14*(4/5), 4–12, doi:10.1130/1052-5173(2004)014<0004:APAOMO>2.0.CO.

Gurenko, A. A., R. B. Trumbull, R. Thomas, and J. M. Lindsay (2005), A melt inclusion record of volatiles, trace elements and LiB isotope variations in a single magma system from the Plat Pays volcanic complex, Dominica, Lesser Antilles, *J. Petrol.*, *46*(12), 2495–2526, doi:10.1093/petrology/egi063.

Halama, R., G. Boudon, B. Villemant, J. L. Joron, A. Le Friant, and J. C. Komorowski (2006), Pre-eruptive crystallization conditions of mafic and silicic magmas at the Plat Pays volcanic complex, Dominica (Lesser Antilles), *J. Volcanol. Geotherm. Res.*, *153*(3–4), 200–220, doi:10.1016/j.jvolgeores.2005.12.001.

Harford, C., M. Pringle, R. Sparks, and S. Young (2002), The volcanic evolution of Montserrat using $^{40}Ar/^{39}Ar$ geochronology, *Geol. Soc. London Mem.*, *21*(1), 93–113, doi:10.1144/GSL.MEM.2002.021.01.05.

Harrison, T. M., E. B. Watson, and A. B. Aikman (2007), Temperature spectra of zircon crystallization in plutonic rocks, *Geology*, *35*(7), 635–638, doi:10.1130/G23505A.1.

Heath, E., S. P. Turner, R. Macdonald, C. J. Hawkesworth, and P. van Calsteren (1998), Long magma residence times at an island arc volcano (Soufriere, St. Vincent) in the Lesser Antilles: Evidence from ^{238}U–^{230}Th isochron dating, *Earth Planet. Sci. Lett.*, *160*(1–2), 49–63, doi:10.1016/S0012-821X(98)00084-3.

Heyworth, Z., S. Turner, B. Schaefer, B. Wood, R. George, K. Berlo, H. Cunningham, R. Price, C. Cook, and J. Gamble (2007), ^{238}U–^{230}Th–^{226}Ra–^{210}Pb constraints on the genesis of high-Mg andesites at White Island, New Zealand, *Chem. Geol.*, *243*(1–2), 105–121, doi:10.1016/j.chemgeo.2007.05.01.2.

Hildreth, W. (2004), Volcanological perspectives on Long Valley, Mammoth Mountain, and Mono Craters: Several contiguous but discrete systems, *J. Volcanol. Geotherm. Res.*, *136*(3), 169–198, doi:10.1016/j.jvolgeores.2004.05.019.

Holbrook, S. W., D. Lizarralde, S. McGeary, N. Bangs, and J. Diebold (1999), Structure and composition of the Aleutian island arc and implications for continental crustal growth, *Geology*, *27*(1), 31–34, doi:10.1130/0091-7613(1999)027<0031:SACOTA>.

Hoskin, P., and U. Schaltegger (2003), The composition of zircon and igneous and metamorphic petrogenesis, *Rev. Mineral. Geochem.*, *53*(1), 27–62, doi:10.1046/j.1525-1314.2000.00266.x.

Howe, T. M., J. Lindsay, P. Shane, A. K. Schmitt, and D. Stockli (2014), Re-evaluation of the Roseau Tuff eruptive sequence and other ignimbrites in Dominica, Lesser Antilles, *J. Quat. Sci.*, *29*(6), 531–546, doi:10.1002/jqs.2723.

Huang, F., C. C. Lundstrom, H. Sigurdsson, and Z. Zhang (2011), U-series disequilibria in Kick'em Jenny submarine volcano lavas: A new view of time-scales of magmatism in convergent margins, *Geochim. Cosmochim. Acta*, *75*(1), 195–212, doi:10.1016/j.gca.2010.05.036.

Iyer, H., J. Evans, P. Dawson, D. Stauber, and U. Achauer (1990), Differences in magma storage in different volcanic environments as revealed by seismic tomography: Silicic volcanic centers and subduction-related volcanoes, in *Magma Transport Storage*, edited by M. P. Ryan, pp. 293–316, John Wiley & Sons, U. K.

Kent, A. J. R., C. Darr, A. M. Koleszar, M. J. Salisbury, and K. M. Cooper (2010), Preferential eruption of andesitic magmas through recharge filtering, *Nat. Geosci.*, *3*(9), 631–636, doi:10.1038/ngeo924.

Kerr, A. C., R. V. White, P. M. E. Thompson, J. Tarney, and A. D. Saunders (2003), No oceanic plateau—no Caribbean Plate? The seminal role of an oceanic plateau in Caribbean plate evolution, in *The Circum-Gulf of Mexico and Caribbean: Hydrocarbon Habitats, Basin Formation, and Plate Tectonics*, edited by C. Bartolini, R. T. Buffler, and J. Blickwede, pp. 126–168, APPG, Memoir 79, Washington, D. C.

Klemetti, E. W., and M. A. Clynne (2014), Localized rejuvenation of a crystal mush recorded in zircon temporal and compositional variation at the Lassen Volcanic Center, Northern California, *PLoS One*, doi:10.1371/journal.pone.0113157.

Kodaira, S., T. Sato, N. Takahashi, A. Ito, Y. T. Tamura, Y., and Y. Kaneda (2007), Seismological evidence for variable growth of crust along the Izu intra-oceanic arc, *J. Geophys. Res.*, *112*, B05104, doi:10.1029/2006JB004593.

Kopp, H., et al. (2011), Deep structure of the central Lesser Antilles Island Arc: Relevance for the formation of continental crust, *Earth Planet. Sci. Lett.*, *304*(1–2), 121–134, doi:10.1016/j.epsl.2011.01.024.

Leat, P. T., and R. D. Larter (2003), Intra-oceanic subduction systems: Introduction, *Geol. Soc. Spec. Publ.*, *219*(1), 1–17, doi:10.1144/GSL.SP.2003.219.01.01.

Le Friant, A., G. Boudon, J. C. Komorowski, and C. Deplus (2002), L'île de la Dominique, à l'origine des avalanches de débris les plus volumineuses de l'arc des Petites Antilles. The Island of Dominica, site for the generation of the most voluminous debris avalanches in the Lesser Antilles Arc, *C. R. Geosci.*, *334*(4), 235–243, doi:10.1016/S1631-0713(02)01742-X.

Lindsay, J., M. Stasiuk, and J. Shepherd (2003), Geological history and potential hazards of the late-Pleistocene to Recent Plat Pays volcanic complex, Dominica, Lesser Antilles, *Bull. Volcanol.*, *65*(2), 201–220, doi:10.1007/s00445-002-0253-y.

Lindsay, J., R. B. Trumbull, and W. Siebel (2005a), Geochemistry and petrogenesis of late Pleistocene to recent volcanism in Southern Dominica, Lesser Antilles, *J. Volcanol. Geotherm. Res.*, *148*(3–4), 253–294, doi:10.1016/j.jvolgeores.2005.04.018.

Lindsay, J., R. Robertson, B. Shepherd, and S. Ali (Eds.) (2005b), *Volcanic Hazard Atlas of the Lesser Antilles*, 279 p., Seismic Res. Cent., St. Augustine, Trinidad and Tobago.

Lowenstern, J. B., H. M. Persing, J. L. Wooden, M. Lanphere, J. Donnelly-Nolan, and T. L. Grove (2000), U–Th dating of single zircons from young granitoid xenoliths: New tools for understanding volcanic processes, *Earth Planet. Sci. Lett.*, *183*(1–2), 291–302, doi:10.1016/S0012-821X(00)00273-9.

Macdonald, R., C. J. Hawkesworth, and E. Heath (2000), The Lesser Antilles volcanic chain: A study in arc magmatism, *Earth Sci. Rev.*, *49*(1–4), 1–76, doi:10.1016/S0012-8252(99)00069-0.

Mahood, G. A. (1990), Second reply to comment of RSJ Sparks, HE Huppert and CJN Wilson on "Evidence for long residence times of rhyolitic magma in the Long Valley magmatic system: The isotopic record in the precaldera lavas of Glass Mountain," *Earth Planet. Sci. Lett.*, *99*(4), 395–399, doi:10.1016/0012-821X(90)90145-N.

Miller, J. S., and J. L. Wooden (2004), Residence, resorption and recycling of zircons in Devils Kitchen Rhyolite, Coso Volcanic Field, California, *J. Petrol.*, *45*(11), 2155–2170, doi:10.1093/petrology/egh051.

Miller, J. S., J. E. P. Matzel, C. F. Miller, S. D. Burgess, and R. B. Miller (2007), Zircon growth and recycling during the assembly of large, composite arc plutons, *J. Volcanol. Geotherm. Res.*, *167*(1–4), 282–299, doi:10.1016/j.jvolgeores.2007.04.019.

Paces, J. B., and J. D. Miller (1993), Precise U-Pb ages of Duluth Complex and related mafic intrusions, northeastern Minnesota: Geochronological insights to physical, petrogenetic, paleomagnetic, and tectonomagmatic processes associated with the 1.1 Ga midcontinent rift system, *J. Geophys. Res.*, *98*(B8), 13,997–14,013, doi:10.1029/93JB01159.

Pedersen, R., M. Searle, A. Carter, and P. Bandopadhyay (2010), U–Pb zircon age of the Andaman ophiolite: Implications for the beginning of subduction beneath the Andaman–Sumatra arc, *J. Geol. Soc.*, *167*(6), 1105–1112, doi:10.1144/0016-76492009-151.

Press, W. H., S. A. Teukolsky, W. T. Vetterling, and B. P. Flannery (1992), *Numerical Recipes in C: The Art of Scientific Computing*, 2nd ed., 994 p., Cambridge Univ. Press, London, U. K.

Rao, T. R. (2008), Geological evolution of the Caribbean plate: Some critical aspects in the two divergent models, *Curr. Sci.*, *95*(6), 736–742.

Reid, M., and C. Coath (2000), In situ U-Pb ages of zircons from the Bishop Tuff: No evidence for long crystal residence times, *Geology*, *28*(5), 443–446, doi:10.1130/0091-7613(2000).

Rioux, M., B. Hacker, J. Mattinson, P. Kelemen, J. Blusztajn, and G. Gehrels (2007), Magmatic development of an intra-oceanic arc: High-precision U-Pb zircon and whole-rock isotopic analyses from the accreted Talkeetna arc, south-central Alaska, *Geol. Soc. Am. Bull.*, *119*(9–10), 1168–1184, doi:10.1130/B25964.1.

Roobol, M. J., J. V. Wright, and A. L. Smith (1983), Calderas or gravity-slide structures in the Lesser Antilles island arc?, *J. Volcanol. Geotherm. Res.*, *19*(1–2), 121–134, doi:10.1016/0377-0273(83)90128-2.

Samper, A., X. Quidelleur, G. Boudon, A. Le Friant, and J. C. Komorowski (2008), Radiometric dating of three large volume flank collapses in the Lesser Antilles Arc, *J. Volcanol. Geotherm. Res.*, *176*(4), 485–492, doi:10.1016/j.jvolgeores.2008.04.018.
Sañudo-Wilhelmy, S. A., and A. R. Flegal (1994), Temporal variations in lead concentrations and isotopic composition in the Southern California Bight, *Geochim. Cosmochim. Acta*, *58*(15), 3315–3320, doi:10.1016/0016-7037(94)90060-4.
Schaltegger, U., G. Zeilinger, M. Frank, and J. P. Burg (2002), Multiple mantle sources during island arc magmatism: U–Pb and Hf isotopic evidence from the Kohistan arc complex, Pakistan, *Terra Nova*, *14*(6), 461–468, doi:10.1046/j.1365-3121.2002.00432.x.
Schmitt, A. K., M. Grove, T. M. Harrison, O. Lovera, J. Hulen, and M. Walters (2003), The Geysers-Cobb Mountain Magma System, California (Part 1): U-Pb zircon ages of volcanic rocks, conditions of zircon crystallization and magma residence times, *Geochim. Cosmochim. Acta*, *67*(18), 3423–3442, doi:10.1016/S0016-7037(03)00140-6.
Schmitt, A. K., D. F. Stockli, and B. P. Hausback (2006), Eruption and magma crystallization ages of Las Tres Virgenes (Baja California) constrained by combined ^{230}Th/^{238}U and (U-Th)/He dating of zircon, *J. Volcanol. Geotherm. Res.*, *158*(3–4), 281–295, doi:10.1016/j.jvolgeores.2006.07.005.
Schmitt, A. K., D. F. Stockli, S. Niedermann, O. M. Lovera, and B. P. Hausback (2010a), Eruption ages of Las Tres Vírgenes volcano (Baja California): A tale of two helium isotopes, *Quat. Geochronol.*, *5*(5), 503–511, doi:10.1016/j.quageo.2010.02.004.
Schmitt, A. K., D. F. Stockli, J. M. Lindsay, R. Robertson, O. M. Lovera, and R. Kislitsyn (2010b), Episodic growth and homogenization of plutonic roots in arc volcanoes from combined U–Th and (U–Th)/He zircon dating, *Earth Planet. Sci. Lett.*, *295*(1–2), 91–103, doi:10.1016/j.epsl.2010.03.028.
Scholl, D. W., and R. von Huene (2009), Implications of estimated magmatic additions and recycling losses at the subduction zones of accretionary (non-collisional) and collisional (suturing) orogens, *Geol. Soc. Spec. Publ.*, *318*(1), 105–125, doi:10.1144/SP318.4.
Sigurdsson, H. (1972), Partly-welded pyroclast flow deposits in Dominica, Lesser Antilles, *Bull. Volcanol.*, *36*(1), 148–163, doi:10.1007/BF02596987.
Smith, A. L., M. J. Roobol, G. S. Mattioli, J. E. Fryxell, G. E. Daly, and L. A. Fernandez (2013), *The Volcanic Geology of the Mid-Arc Island of Dominica, Lesser Antilles: The Surface Expression of an Island-Arc Batholith*, Geol. Soc. of Am., Boulder, Colo.
Smyth, H. R., P. J. Hamilton, R. Hall, and P. D. Kinny (2007), The deep crust beneath island arcs: Inherited zircons reveal a Gondwana continental fragment beneath East Java, Indonesia, *Earth Planet. Sci. Lett.*, *258*(1–2), 269–282, doi:10.1016/j.epsl.2007.03.044.
Sparks, R. S. J., H. Sigurdsson, and S. N. Carey (1980), The entrance of pyroclastic flows into the sea I. Oceanographic and geologic evidence from Dominica, Lesser Antilles, *J. Volcanol. Geotherm. Res.*, *7*(1–2), 87–96, doi:10.1016/0377-0273(80)90021-9.
Storm, S., P. Shane, A. Schmitt, and J. Lindsay (2012), Decoupled crystallization and eruption histories of the rhyolite magmatic system at Tarawera volcano revealed by zircon ages and growth rates, *Contrib. Mineral. Petrol.*, *163*(3), 505–519, doi:10.1007/s00410-011-0682-8.
Takahashi, N., S. Kodaira, Y. Tatsumi, Y. Kaneda, and K. Suyehiro (2008), Structure and growth of the Izu-Bonin-Mariana arc crust: 1. Seismic constraint on crust and mantle structure of the Mariana arc–back-arc system, *J. Geophys. Res.*, *113*, B01104, doi:10.1029/2007JB005120.
Tamura, Y., et al. (2009), Silicic Magmas in the Izu-Bonin oceanic arc and implications for crustal evolution, *J. Petrol.*, *50*(4), 685–723, doi:10.1093/petrology/egp017.
Tatsumi, Y., and S. M. Eggins (1995), *Subduction Zone Magmatism*, 211 p., Blackwell Sci., Cambridge, Mass.
Taylor, S. R. (1967), The origin and growth of continents, *Tectonophysics*, *4*(1), 17–34, doi:10.1016/0040-1951(67)90056-X.
Toothill, J., C. A. Williams, R. MacDonald, S. P. Turner, N. W. Rogers, C. J. Hawkesworth, D. A. Jerram, C. J. Ottley, and A. G. Tindle (2007), A complex petrogenesis for an arc magmatic suite, St Kitts, Lesser Antilles, *J. Petrol.*, *48*(1), 3–42, doi:10.1093/petrology/egl052.
Turner, S., C. Hawkesworth, P. van Calsteren, E. Heath, R. Macdonald, and S. Black (1996), U-series isotopes and destructive plate margin magma genesis in the Lesser Antilles, *Earth Planet. Sci. Lett.*, *142*(1–2), 191–207, doi:10.1016/0012-821X(96)00078-7.
Turner, S., J. Caulfield, T. Rusher, M. Turner, S. Cronin, I. Smith, and H. Handley (2012), Magma evolution in the primitive, intra-oceanic Tonga Arc: Rapid petrogenesis of dacties at Fonualei volcano, *J. Petrol.*, *53*(6), 1231–1253, doi:10.1093/petrology/egs005.
Vogel, T. A., L. C. Patino, G. E. Alvarado, and P. B. Gans (2004), Silicic ignimbrites within the Costa Rican volcanic front: Evidence for the formation of continental crust, *Earth Planet. Sci. Lett.*, *226*, 149–159, doi:10.1016/j.epsl.2004.07.013.
Wade, J. A., et al. (2005), The May 2003 eruption of Anatahan volcano, Mariana Islands: Geochemical evolution of a felsic island-arc volcano, *J. Volcanol. Geotherm. Res.*, *146*, 139–170, doi:10.1016/j.jvolgeores.2004.11.035.
Ward, K. M., G. Zandt, S. L. Beck, D. H. Christensen, and H. McFarlin (2014), Seismic imaging of the magmatic underpinnings beneath the Altiplano-Puna volcanic complex from the joint inversion of surface wave dispersion and receiver functions, *Earth Planet. Sci. Lett.*, *404*, 43–53, doi:10.1016/j.epsl.2014.07.022.
Watson, E. B., and T. M. Harrison (1983), Zircon saturation revisited: Temperature and composition effects in a variety of crustal magma types, *Earth Planet. Sci. Lett.*, *64*(2), 295–304, doi:10.1016/0012-821X(83)90211-X.
White, S. M., J. A. Crisp, and F. J. Spera (2006), Long-term volumetric eruption rates and magma budgets, *Geochem. Geophys. Geosyst.*, *7*, Q03010, doi:10.1029/2005GC001002.
Whitham, A. G. (1989), The behaviour of subaerially produced pyroclastic flows in a subaqueous environment: Evidence from the Roseau eruption, Dominica, West Indies, *Mar. Geol.*, *86*(1), 27–40, doi:10.1016/0025-3227(89)90016-9.
Wilson, C. J. N., and B. L. A. Charlier (2009), Rapid rates of magma generation at contemporaneous magma systems, Taupo Volcano, New Zealand: Insights from UTh model-age spectra in zircons, *J. Petrol.*, *50*(5), 875–907, doi:10.1093/petrology/egp023.
Zellmer, G. F., C. J. Hawkesworth, R. S. J. Sparks, L. E. Thomas, C. L. Harford, T. S. Brewer, and S. C. Loughlin (2003), Geochemical evolution of the Soufrière Hills Volcano, Montserrat, Lesser Antilles Volcanic Arc, *J. Petrol.*, *44*(8), 1349–1374, doi:10.1093/petrology/44.8.1349.

Erratum

In the originally published version of this article, some data in Table 1 was typeset on the wrong lines. The data have since been corrected and this version may be considered the authoritative version of record.